Supporting Information

Synthesis of α-amino nitriles through one-pot selective Ru-photocatalyzed oxidative cyanation of amines

Igor Echevarría,[a] Mónica Vaquero,[a] Roberto Quesada[a] and Gustavo Espino*[a]

[a]*Departamento de Química, Facultad de Ciencias, Universidad de Burgos, Plaza Misael Bañuelos s/n, 09001, Burgos, Spain.*

Table of Contents

1.- General Information

All synthetic manipulations were carried out under an atmosphere of dry, oxygen-free nitrogen using standard Schlenk techniques. The solvents were dried and distilled under nitrogen atmosphere before use. Elemental analyses were performed with a Thermo Fisher Scientific EA Flash 2000 Elemental Microanalyzer. The disagreement between calculated and found values for carbon of complexes **[Ru1]Cl_2-[Ru5]Cl_2** was slightly > 0.4%, so that fraction of solvent molecules (H_2O) were introduced in the molecular formulae to improve agreement. IR spectra were recorded on a Jasco FT/IR-4200 spectrophotometer (4000–400 cm^{-1} range) with Single Reflection ATR Measuring Attachment. UV-Vis absorption was measured in an Evolution 300 UV-Vis double beam spectrophotometer (Thermo Scientific). Fluorescence steady-state and lifetime measurements were performed in a FLS980 (Edinburg Instruments) Fluorimeter with Xenon Arc Lamp 450W and TCSPC laser, respectively. Quantum Yield was determined by using in a FLS980 (Edinburg Instruments) with Xenon Arc Lamp 450W and Red PMT Sphere as detector. HR-ESI(+) Mass spectra (position of the peaks in Da) were recorded with an Agilent LC-MS system (1260 Infinity LC / 6545 Q-TOF MS spectrometer) using DCM/DMSO (4:1) as the sample solvent and (0.1%) aqueous HCOOH/MeOH as the mobile phase. The experimental *m/z* values are expressed in Da compared with the *m/z* values for monoisotopic fragments. NMR samples were prepared by dissolving the suitable amount of compound in 0.5 mL of the respective deuterated solvent and the spectra were recorded at 298 K on a Varian Unity Inova-400 (399.94 MHz for ^1H; 376.29 MHz for ^{19}F; 100.6 MHz for ^{13}C). Typically, ^1H NMR spectra were acquired with 32 scans into 32 k data points over a spectral width of 16 ppm. ^1H and $^{13}C\{^1H\}$ chemical shifts were internally referenced to TMS via the residual ^1H and ^{13}C signals of DMSO-d_6 (δ = 2.50 ppm and δ = 39.52 ppm), CD_3CN (δ = 1.94 ppm and δ = 118.69 (-CN) and 1.39 (-CD_3) ppm) and $CDCl_3$ (δ = 7.26 ppm and δ = 77.16 ppm), according to the values reported by Fulmer et al.[1] Chemical shift values (δ) are reported in ppm and coupling constants (*J*) in Hertz. The splitting of proton resonances in the reported ^1H NMR data is defined as s = singlet, d = doublet, t = triplet, q = quartet, m = multiplet, bs = broad singlet. 2D NMR spectra such as ^1H-^1H gCOSY, ^1H-^1H NOESY, ^1H-^{13}C gHSQC and ^1H-^{13}C gHMBC were recorded using standard pulse sequences. The probe temperature ($\pm$1 K) was controlled by a standard unit calibrated with methanol as a reference. All NMR data processing was carried out using MestReNova version 10.0.2.

Starting materials. $RuCl_3 \cdot x\ H_2O$ was purchased from Johnson Matthey and used as received. The starting dimer $[Ru(bpy)_2Cl_2] \cdot 2H_2O$ (bpy = 2,2'-bipyridine) was prepared according to the reported procedure.[2] The reagents 2,2'-bipyridine, iodomethane and benzyl bromide were purchased from Sigma-Aldrich; 2-(2-pyridyl)benzimidazole and 4-iodobenzyl bromide were purchased from Acros Organics-Fisher Scientific, and 2-(bromomethyl)naphthalene was purchased from Alfa Aesar. All of them were used without further purification. Deuterated solvents (DMSO-d_6, $CDCl_3$, CD_3CN) were obtained from Eurisotop. Conventional solvents such as diethyl ether (Fisher Scientific), acetone (Fisher Scientific) and 2-ethoxyethanol (Across Organics) were degassed and in some cases distilled prior to use. Acetonitrile used in the photocatalytic experiments were acquired from a Fisher Scientific (HPLC quality). Tetrabutylammonium hexafluorophosphate ($[^nBu_4N][PF_6]$) was purchased from Acros. Synthetic procedure of the ligands was previously described in the literature: **L2**,[3] **L3**,[4] **L4**3 and **L5**.[5]

2.- Synthesis and characterization of the Ru(II)-complexes

---

[1] G. R. Fulmer, A. J. M. Miller, N. H. Sherden, H. E. Gottlieb, A. Nudelman, B. M. Stoltz, J. E. Bercaw, K. I. Goldberg, *Organometallics* **2010**, *29*, 2176–2179.
[2] G. Sprintschnik, H. W. Sprintschnik, P. P. Kirsch and D. G. Whitten, *J. Am. Chem. Soc.*, **1977**, *99*, 4947–4954
[3] J.A. Maynard, I.D. Rae, D. Rash, J.M. Swan, *Aust. J. Chem.*, **1971***, 24*, 1873-1881.
[4] W.-K. Huang, C.-W. Cheng, S.-M. Chang, Y.-P. Lee, E. W.-G. Diau, *Chem. Commun.* **2010**, *46*, 8992–8994.
[5] N. M. Shavaleev, Z. R. Bell, T. L. Easun, R. Rutkaite, M. D. Ward. *Dalton Trans.* **2004**, 3678–3688.

Synthesis of $[Ru(bpy)_2(L1)]Cl_2$: [Ru1]Cl_2

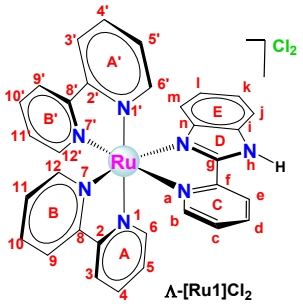

In a 100 mL Schlenk flask, the ancillary ligand **L1** (0.037 g, 0.193 mmol) was added to a solution of $RuCl_2(bpy)_2{\cdot}2H_2O$ (0.100 g, 0.193 mmol) in EtOH (19 mL), and the mixture was stirred at 90 °C for 16 h. Then, the volume was reduced to the half under vacuum and Et_2O (15 mL) was added to precipitate a dark red solid that was isolated by filtration and washed with Et_2O (5 mL). Then, the solid was dried under vacuum at 80 °C for 6 h. Dark red powder. Yield: 0.081 g (0.119 mmol, 62%).**^{1}H NMR (400 MHz, DMSO-d$_6$, 25 °C)** δ 16.20 (s, 1H; H^{N-H}), 9.06 (d, J_{H-H} = 7.7 Hz, 1H; H^e), 8.88 (dd, J_{H-H} = 8.1, 4.1 Hz, 3H; H^9, $H^{9'}$, H^3), 8.80 (d, J_{H-H} = 8.1 Hz, 1H; $H^{3'}$), 8.24 (t, J_{H-H} = 7.9 Hz, 2H; H^d, H^4), 8.15 (dt, J_{H-H} = 10.6, 7.6 Hz, 2H; H^{10}, $H^{10'}$), 8.08 (t, J_{H-H} = 7.5 Hz, 1H; $H^{4'}$), 7.96 (d, J_{H-H} = 5.7 Hz, 1H; H^6), 7.85 (d, J_{H-H} = 5.7 Hz, 1H; $H^{12'}$), 7.82 – 7.76 (m, 2H, H^{12}, $H^{6'}$), 7.74 (d, J = 8.3 Hz, 1H, H^b), 7.70 (d, J = 5.6 Hz, 1H, H^j), 7.63 – 7.57 (m, 1H, H^c), 7.52 (dq, J = 13.5, 6.6 Hz, 4H, H^5, H^{11}, $H^{11'}$, $H^{5'}$), 7.36 (t, J = 7.7 Hz, 1H, H^k), 7.02 (t, J = 7.8 Hz, 1H, H^l), 5.65 (d, J = 8.3 Hz, 1H, H^m) ppm. **^{13}C{^{1}H} NMR** spectra data is not available due to decomposition signs observed in DMSO-d$_6$. **FT-IR (ATR) selected bands:** 3376 (w, ν_{N-H}), 3012 (w, $\nu_{C=CH}$), 1602-1541 (m, $\nu_{C=C\ +\ C-N}$), 1419 (w, $\nu_{C=N}$), 1151 (m, ν_{C-C}), 1065-1023 (m, δ_{C-Hip}), 764-730 (vs, δ_{C-Hoop}). **HR-MS ESI(+)(DCM/DMSO, 4:1):** $[M-H^+]^+$ calcd. for $[C_{32}H_{24}N_7Ru]^+$ 608.1137; found 608.1145; $[M]^{2+}$ calcd. for $[C_{32}H_{25}N_7Ru]^{2+}$ 304.5602 found 304.5612 Da. **Anal. Calcd for $C_{32}H_{25}Cl_2N_7Ru(H_2O)_{0.35}$:** C 56.04; H 3.78; N 14.29; **Found:** C 56.25; H 4.01; N 14.25.

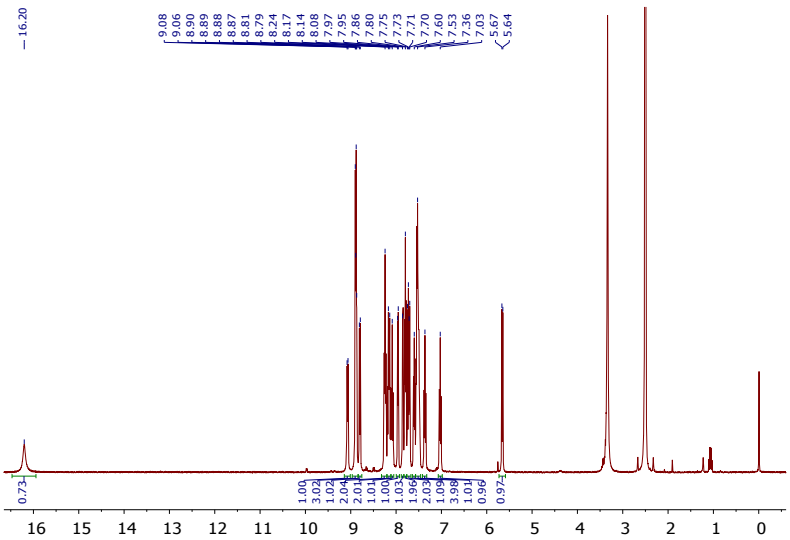

Figure SI1. ^{1}H NMR (400 MHz, DMSO-d$_6$, 25 °C) spectrum of **[Ru1]Cl_2**.

Synthesis of $[Ru(bpy)_2(L2)]Cl_2$, $[Ru_2]Cl_2$

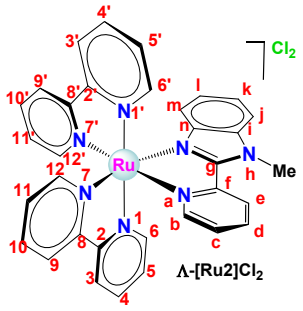

In a 100 mL Schlenk flask, the ancillary ligand **L2** (0.040 g, 0.192 mmol) was added to a solution of $RuCl_2(bpy)_2 \cdot 2H_2O$ (0.100 g, 0.192 mmol) in ethanol (19 mL), and the mixture was stirred at 90 °C for 16 h. Then, the volume was reduced to the half under vacuum and diethyl ether (15 mL) was added to precipitate a crude solid that was isolated by filtration and washed with diethyl ether (5 mL). The solid was dissolved in methanol/acetone 1:1 (0.75 mL:0.75 mL) and placed in the freezer for 2 days to precipitate the excess of precursor. Then the solution was filtered, the solvent was removed under vacuum and the resulting solid was washed with Et_2O (5 mL), and dried under vacuum at 80 °C for 6 h. Dark Red solid. Yield: 0.041 g (0.059 mmol, 31%). **^{1}H NMR (400 MHz, DMSO-d$_6$, 25 °C)** δ 8.91 (d, J_{H-H} = 8.2 Hz, 3H; H^3, H^9, $H^{9'}$), 8.81 (dd, J_{H-H} = 8.2, 4.3 Hz, 2H; $H^{3'}$, H^e), 8.24 (m, 2H; H^4, H^{10}), 8.15 (m, 2H; $H^{10'}$, $H^{4'}$), 8.09 (td, J_{H-H} = 7.9, 1.2 Hz, 1H; H^d), 8.01 (d, J_{H-H} = 8.5 Hz, 1H; H^j), 7.91 (d, J_{H-H} = 5.0 Hz, 1H; H^6), 7.82 (d, J_{H-H} = 5.5 Hz, 1H; $H^{6'}$), 7.79 (d, J_{H-H} = 5.57 Hz, 2H; H^b or $H^{12'}$), 7.77 (d, J_{H-H} = 5.2 Hz, 2H; H^b or $H^{12'}$), 7.73 (d, J_{H-H} = 5.1 Hz, 1H; H^{12}), 7.57 (m, 4H; H^5, $H^{5'}$, H^{11}, $H^{11'}$), 7.46 (m, 2H; H^c, H^k), 7.08 (t, J_{H-H} = 7.8 Hz, 1H; H^l), 5.68 (d, J_{H-H} = 8.4 Hz, 1H; H^m), 4.47 (s, 3H; H^{N-Me}) ppm. **^{13}C{^{1}H} NMR** spectra data is not available due to decomposition signs observed in DMSO-d$_6$. **FT-IR (ATR) selected bands:** 3063 (w, $\nu_{C=CH}$), 1601-1565 (m, $\nu_{C=C+C-N}$), 1420 (w, $\nu_{C=N}$), 1162 (m, ν_{C-C}), 1025 (m, δ_{C-Hip}), 806 (w, δ_{C-C}), 745-731 (vs, δ_{C-Hoop}). **HR-MS ESI(+)(DCM/DMSO, 4:1):** m/z $[M-Me]^+$ calcd. for $[C_{32}H_{24}N_7Ru]^+$ 608.1131 found 608.1140 Da; $[M-$**L2**$+Cl^-]^+$ calcd. for $[C_{20}H_{16}N_4RuCl]^+$ 449.0102; found 449.0106 Da; $[M]^{2+}$ calcd. for $[C_{33}H_{27}N_7Ru]^{2+}$ 311.5680; found 311.5693. **Anal. Calcd for $C_{33}H_{27}Cl_2N_7Ru(H_2O)_{0.32}$:** C 56.67; H 3.98; N 14.02; **Found:** C 56.80; H 4.13; N 14.29.

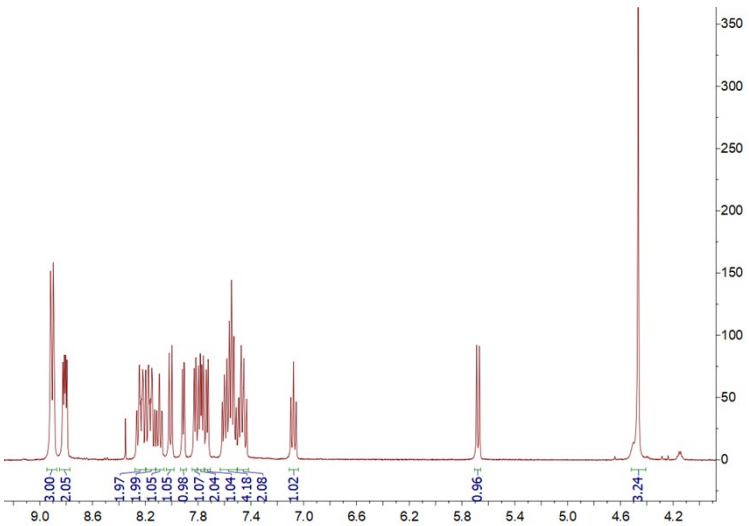

Figure SI2. ^{1}H NMR (400 MHz, DMSO-d$_6$, 25 °C) spectrum of **$[Ru2]Cl_2$**.

Synthesis of $[Ru(bpy)_2(L3)]Cl_2$, $[Ru3]Cl_2$

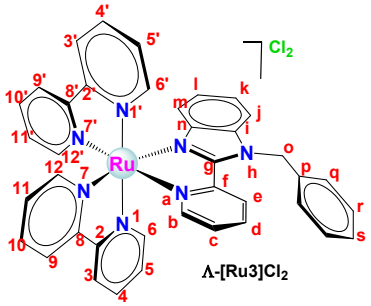

In a 100 mL Schlenk flask, the ancillary ligand **L3** (0.055 g, 0.193 mmol) was added to a solution of $RuCl_2(bpy)_2{\cdot}2H_2O$ (0.100 g, 0.192 mmol) in ethanol (19 mL), and the mixture was stirred at 90 °C for 24 h. Then, the volume was reduced to the half under vacuum and diethyl ether (15 mL) was added to precipitate a crude solid that was isolated by filtration and washed with diethyl ether (5 mL). The solid was dissolved in water, filtered and dried under vacuum. The solid was washed with diethyl ether (5 mL) and dried under vacuum at 80 °C for 6 h. Dark red solid. Yield: 0.083 g (0.107 mmol, 56%). **^{1}H NMR (400 MHz, DMSO-d$_6$, 25 °C)** δ 8.93 (br s, 3H; H^3, H^9, $H^{9'}$), 8.85 (d, J_{H-H} = 8.3 Hz; 1H, $H^{3'}$), 8.53 (d, J_{H-H} = 8.3 Hz, 1H; H^e), 8.27 (t, J_{H-H} = 7.9 Hz, 1H; H^4), 8.17 (m, 2H; H^{10}, $H^{10'}$), 8.11 (d, J_{H-H} = 8.3 Hz, 1H; H^b), 8.06 (m, 2H; H^d, $H^{4'}$), 7.97 (d, J_{H-H} = 5.4 Hz, 1H; H^6), 7.88 (d, J_{H-H} = 5.4 Hz, 1H; $H^{6'}$), 7.77 (m, 2H; $H^{12'}$, H^{12}), 7.68 (d, J_{H-H} = 5.4 Hz, 1H; H^j), 7.63 (m, 1H; H^5), 7.50 (m, 5H; H^{11}, $H^{11'}$, $H^{5'}$, H^c, H^k), 7.33 (m, 3H; H^r, H <^{r}, H^s), 7.14 (m, 1H; H^l), 7.05 (s, H^q), 7.03 (s, H^q), 6.37 (d, J_{H-H} = 17.9 Hz, 1H; H^o), 6.29 (d, J_{H-H} = 17.9 Hz, 1H, H^o), 5.76 (d, J = 8.3 Hz, 1H; H^m) ppm. **^{13}C{^{1}H} NMR (101 MHz, DMSO-d$_6$, 25 °C)** δ 157.33, 156.91, 156.46, 152.44, 151.62, 151.20, 151.00, 150.55, 147.73, 139.77, 137.93, 137.72, 137.59, 137.54, 137.41, 136.64, 135.09, 128.95, 127.77, 127.74, 127.63, 127.59, 127.55, 127.43, 126.13, 125.59, 125.38, 125.14, 124.50, 124.37, 124.22, 123.98, 114.87, 112.85, 47.98 ppm. **FT-IR (ATR) selected bands:** 3065 (w, $\nu_{C=CH}$), 1601-1565 (m, $\nu_{C=C\ +\ C-N}$), 1420 (w, $\nu_{C=N}$), 1157 (m, ν_{C-C}), 1062-1015 (m, δ_{C-Hip}), 773 (vs, δ_{C-Hoop}). **HR-MS ESI(+)(DCM/DMSO, 4:1):** m/z $[M-Bn]^+$ calcd. for $[C_{32}H_{24}N_7Ru]^+$ 608.1131; found 608.1138 Da; $[M]^{2+}$ calcd. for $[C_{39}H_{31}N_7Ru]^{2+}$ 349.5837; found 349.5850 Da. **Anal. Calcd for $C_{39}H_{31}Cl_2N_7Ru(H_2O)_{0.85}$:** C 59.67; H 4.20; N 12.49; **Found:** C 59.79; H 4.35; N 12.70

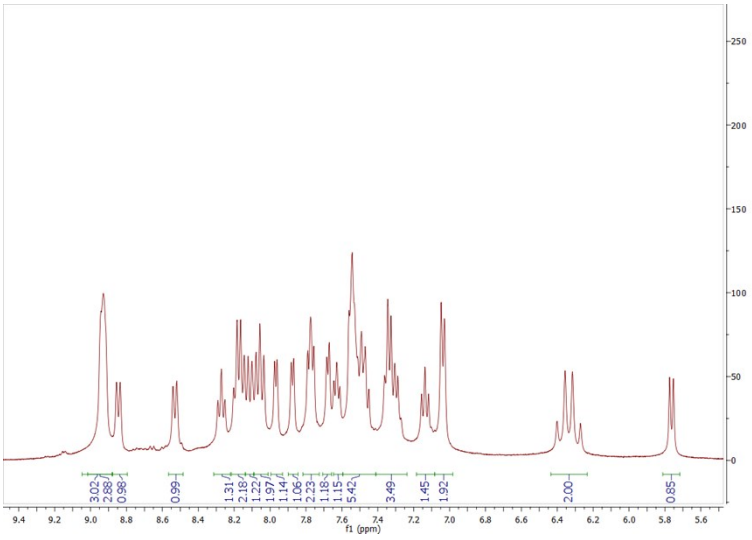

Figure SI3. ^{1}H NMR (400 MHz, DMSO-d$_6$, 25 °C) spectrum of **$[Ru3]Cl_2$.**

Synthesis of $[Ru(bpy)_2(L4)]Cl_2$, $[Ru4]Cl_2$

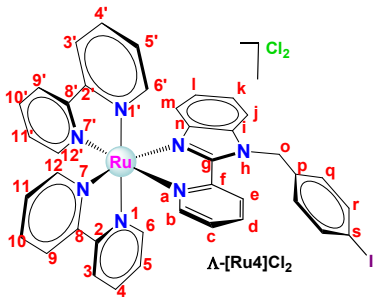

In a 100 mL Schlenk flask, the ancillary ligand **L4** (0.079 g, 0.192 mmol) was added to a solution of $RuCl_2(bpy)_2{\cdot}2H_2O$ (0.100 g, 0.192 mmol) in ethanol (19 mL), and the mixture was stirred at 90 °C for 16 h. Then, the volume was reduced to the half under vacuum and diethyl ether (15 mL) was added to precipitate a crude solid that was isolated by filtration and washed with diethyl ether (5 mL). The solid was dissolved in methanol/acetone 1:1 (0.75/0.75 mL) and placed in the freezer for 2 days. Then the solution was filtered, dried under vacuum, washed with diethyl ether (5 mL) and finally, dried under vacuum at 80 °C for 6h. Dark red solid. Yield: 0.09 g (0.101 mmol, 53%). **^{1}H NMR (400 MHz, DMSO-d$_6$, 25 °C)** δ 8.90 (m, 3H; H^3, H^9, $H^{9'}$), 8.82 (d, J_{H-H} = 8.0 Hz, 1H; $H^{3'}$), 8.46 (d, J_{H-H} = 8.4 Hz, 1H; H^e), 8.27 (t, J_{H-H} = 7.9 Hz, 1H; H^4), 8.17 (q, J_{H-H} = 7.9 Hz, 2H; H^{10}, $H^{10'}$), 8.09 (m, 2H; $H^{4'}$, H^d), 8.01 (d, J_{H-H} = 8.5 Hz, 1H; H^j), 7.96 (d, J_{H-H} = 5.3 Hz, 1H; H^6), 7.85 (d, J_{H-H} = 5.3 Hz, 1H; $H^{12'}$), 7.79 (d, J_{H-H} = 5.2 Hz, 1H; H^{12}), 7.75 (d, J_{H-H} = 5.4 Hz, 1H; $H^{6'}$), 7.72 (s, 1H; H^b), 7.62 (m, 2H;, H^r, H^r), 7.62 (m, 1H; H^5), 7.51 (m, 5;, H^{11}, $H^{11'}$, $H^{5'}$, H^c, H^k), 7.13 (t, J_{H-H} = 7.8 Hz, 1H; H^l), 6.89 (s, 1H; H^q), 6.86 (s, 1H; H^q), 6.32 (d, J_{H-H} = 18.1 Hz, 1H; H^o), 6.24 (d, J_{H-H} = 18.1 Hz, 1H; H^o), 5.75 (d, J = 8.4 Hz, 1H, H^m) ppm. **^{13}C{^{1}H} NMR (101 MHz, DMSO-d$_6$, 25 °C)** δ 157.54, 157.13, 156.66, 156.64, 152.67, 151.78, 151.34, 150.68, 147.83, 139.99, 138.12, 137.84, 137.77, 137.66, 136.72, 135.10, 128.11, 127.84, 126.42, 125.49, 125.39, 124.66, 124.54, 124.13, 115.08, 113.00, 94.23, 47.80 ppm. **FT-IR (ATR) selected bands:** 3066 (w, $\nu_{C=CH}$), 1601-1572 (m, $\nu_{C=C+C-N}$), 1439 (w, $\nu_{C=N}$), 1159 (m, ν_{C-C}), 1060 (m, δ_{C-Hip}), 762-746 (vs, δ_{C-Hoop}). **HR-MS ESI(+)(DCM/DMSO, 4:1):** m/z $[M-(4-I-Bn)]^+$ calcd. for $[C_{32}H_{24}N_7Ru]^+$ 608.1131; found 608.1143; $[M]^{2+}$ calcd. for 412.5320; found 412.5329. **Anal. Calcd for $C_{39}H_{30}Cl_2IN_7Ru(H_2O)_{0.64}$:** C 51.64; H 3.48; N 10.81; **Found:** C 51.69; H 3.60; N 11.03.

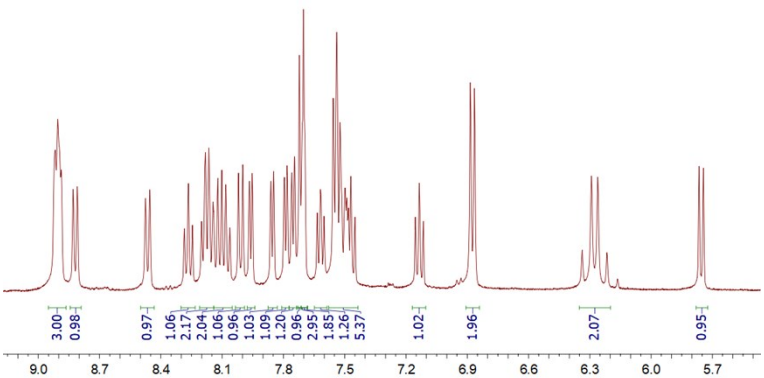

Figure SI4. ^{1}H NMR (400 MHz, DMSO-d$_6$, 25 °C) spectrum of **$[Ru4]Cl_2$**.

Synthesis of $[Ru(bpy)_2(L5)]Cl_2$, $[Ru5]Cl_2$

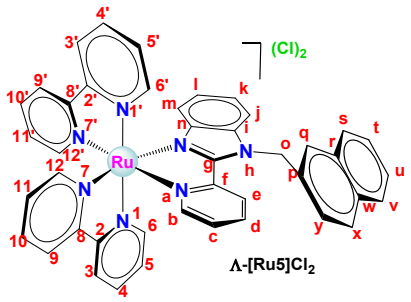

In a 100 mL Schlenk flask, the ancillary ligand **L5** (0.065 g, 0.193 mmol) was added to a solution of $RuCl_2(bpy)_2{\cdot}2H_2O$ (0.100 g, 0.192 mmol) in ethanol (19 mL), and the mixture was stirred at 90 °C for 16 h. Then, the volume was reduced to the half under vacuum and diethyl ether (15 mL) was added to precipitate a crude solid that was isolated by filtration and washed with diethyl ether (5 mL). The solid was dissolved in ethanol/Acetone 1:1 (0.75/0.75 mL) and placed in the freezer for 3 days. Then the solution is filtered, dried under vacuum, washed with diethyl ether (5 mL) and dried under vacuum at 80 °C for 6 h. Dark red solid. Yield: 0.081 g (0.099 mmol, 51%). **^{1}H NMR (400 MHz, DMSO-d$_6$, 25 °C)** δ 8.92 (m, 3H; H^3, H^9, $H^{9'}$), 8.86 (d, J_{H-H} = 7.9 Hz, 1H ;$H^{3'}$), 8.50 (d, J_{H-H} = 8.3 Hz, 1H; H^e), 8.28 (t, J_{H-H} = 7.7 Hz, 1H; H^4), 8.17 (m, 3H; H^{10}, $H^{10'}$, $H^{4'}$), 8.09 (d, J_{H-H} = 8.4 Hz, 1H), 8.03 (m, 1H; H^d), 7.97 (m; 3H), 7.91 (m, 1H), 7.74 (m; 4H), 7.64 (m, 1H; H^5), 7.51 (m, 8H; H^{11}, $H^{11'}$, $H^{5'}$, H^c, H^k, $3H_{arom}$), 7.29 (d, J_{H-H} = 8.7 Hz, 1H), 7.16 (t, J_{H-H} = 7.7 Hz, 1H; H^l), 6.52 (d, J_{H-H} = 18.1 Hz, 1H; H^o), 6.42 (d, J_{H-H} = 18.1 Hz, 1H; H^o), 5.79 (d, J_{H-H} = 8.2 Hz, 1H; H^m) ppm. **^{13}C{^{1}H} NMR (101 MHz, DMSO-d$_6$, 25 °C)** δ 157.58, 157.13, 156.69, 152.64, 151.93, 151.84, 151.37, 151.32, 150.81, 147.91, 140.08, 138.13, 137.91, 137.82, 137.75, 137.60, 136.91, 132.96, 132.75, 132.37, 131.45, 129.01, 127.95, 127.87, 127.80, 127.72, 127.67, 127.64, 126.76, 126.44, 126.37, 126.33, 125.55, 125.38, 124.68, 124.55, 124.43, 124.22, 124.15, 123.93, 115.14, 113.12, 48.45 ppm. **FT-IR (ATR) selected bands:** 3065 (w, $\nu_{C=CH}$), 1601-1576 (m, $\nu_{C=C + C-N}$), 1421 (w, $\nu_{C=N}$), 1157 (m, ν_{C-C}), 1062-1013 (m, δ_{C-Hip}), 763-746 (vs, δ_{C-Hoop}). **HR-MS ESI(+)(DCM/DMSO, 4:1):** m/z $[M-(CH_2\text{-Naphtyl})]^+$ calcd. for $[C_{32}H_{24}N_7Ru]^+$ 608.1131; found 608.1130; $[M]^{2+}$ calcd. for $[C_{43}H_{33}N_7Ru]^{2+}$ 374.5915; found 374.5924. **Anal. Calcd for $C_{43}H_{33}Cl_2N_7Ru(H_2O)_{0.75}$:** C 61.98; H 4.17; N 11.77; **Found:** C 61.90; H 4.32; N 12.01.

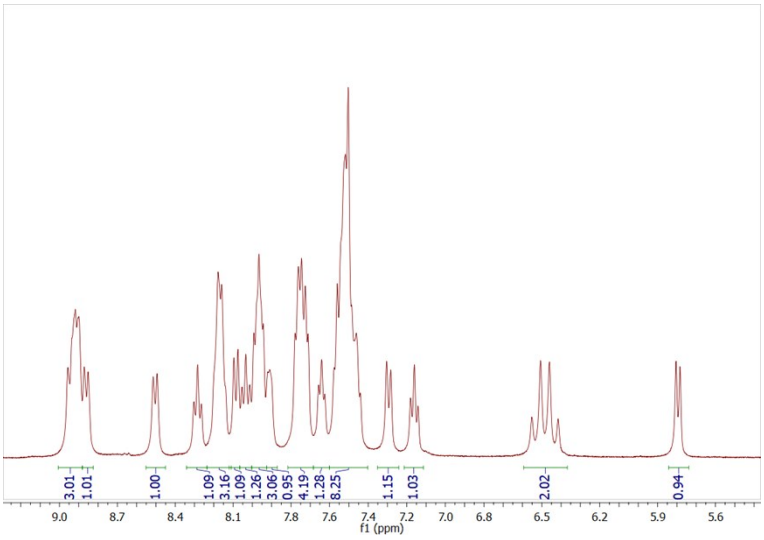

Figure SI5. ^{1}H NMR (400 MHz, DMSO-d$_6$, 25 °C) spectrum of **$[Ru5]Cl_2$**.

3.- X-Ray diffraction: Crystallographic parameters and spatial interactions

Table SI1.- Crystal data and structure refinement for [RuL3](PF_6)$_2$.	
Empirical formula	$C_{39}H_{31}F1_2N_7P_2Ru$
Formula weight	988.72
Temperature/K	299.0
Crystal system	monoclinic
Space group	$P2_1/c$
a/Å	20.7784(11)
b/Å	11.5929(6)
c/Å	16.7092(8)
α/°	90
β/°	97.550(2)
γ/°	90
Volume/Å^3	3990.1(4)
Z	4
ρ_{calc}g/cm^3	1.646
μ/mm^{-1}	0.570
F(000)	1984.0
Crystal size/mm^3	0.3 × 0.1 × 0.1
Radiation	MoKα (λ = 0.71073)
2Θ range for data collection/°	4.586 to 55.444
Index ranges	-27 ≤ h ≤ 26, -15 ≤ k ≤ 15, -20 ≤ l ≤ 21
Reflections collected	64983
Independent reflections	9267 [R_{int} = 0.1518, R_{sigma} = 0.0875]
Data/restraints/parameters	9267/0/551
Goodness-of-fit on F^2	1.090
Final R indexes [I>=2σ (I)]	R_1 = 0.0631, wR_2 = 0.1459
Final R indexes [all data]	R_1 = 0.1576, wR_2 = 0.2238
Largest diff. peak/hole / e Å^{-3}	1.23/-0.85

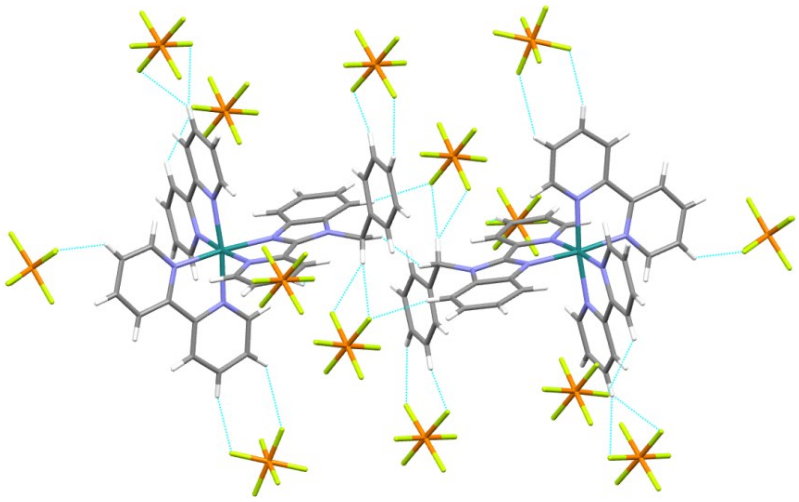

Figure SI6. Intermolecular Hydrogen bonding interactions in the crystal structure of **[Ru3](PF$_6$)$_2$**.

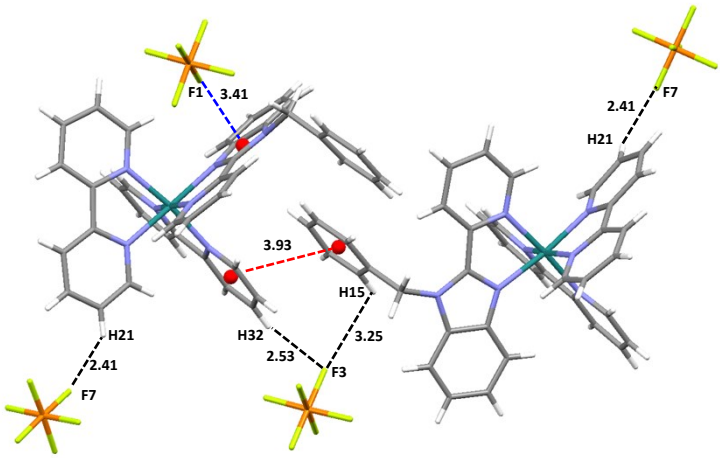

Geometric data for the π···π interaction in complex **[Ru3](PF$_6$)$_2$**				
Groups involved	**Ct–Ct (Å)**	**Ct–pl (Å)**	**α (º)**	**β and γ**
Ring 1: C14–C19 Ring 2: N7,C30–C34	3.93	3.51 (Ct1–pl2) 3.33 (Ct2–pl1)	5.21	26.7 32.1

Ct = centroid, pl = plane. β and γ are the angles formed by the centroid–centroid and centroid–plane lines. α is the dihedral angle formed by the plane of the two rings of the π–π stacking.

Geometric data for the anion···π interaction in complex **[Ru3](PF$_6$)$_2$**			
Groups involved	F-Ct (Å)	F-pl (Å)	β (°)
F$_5$P1–F1···π (Imidazole ring, N2,N3,C6,C7,C12)	3.41	3.00	28.4

Ct = centroid, pl = plane. β is the angle formed by the H–centroid and H–plane lines.

Figure SI7. Selected non-covalent interactions present in the crystal structure of complex **[Ru3](PF$_6$)$_2$**. π···π interaction in red, anion···π interaction in blue and hydrogen bonds in black. There are more hydrogen bonds that those indicated.

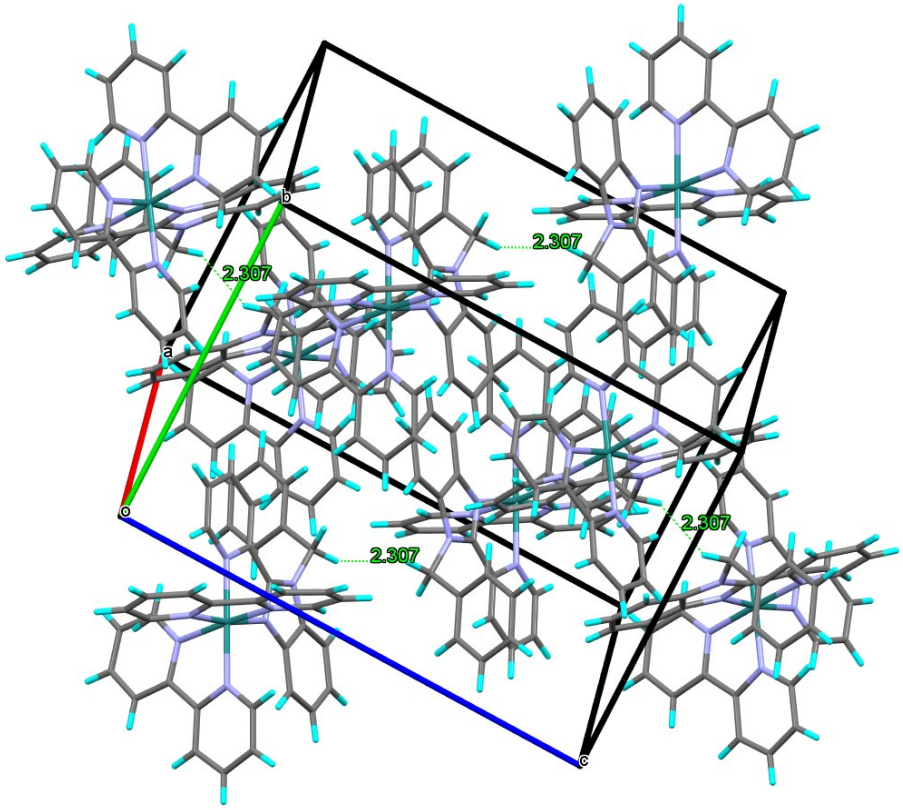

Figure SI8. CH-CH interactions in the unit cell of the crystal structure of **[Ru3](PF_6)$_2$** that involves the CH_2 groups.

4.- Photostability of the Ruthenium(II) complexes

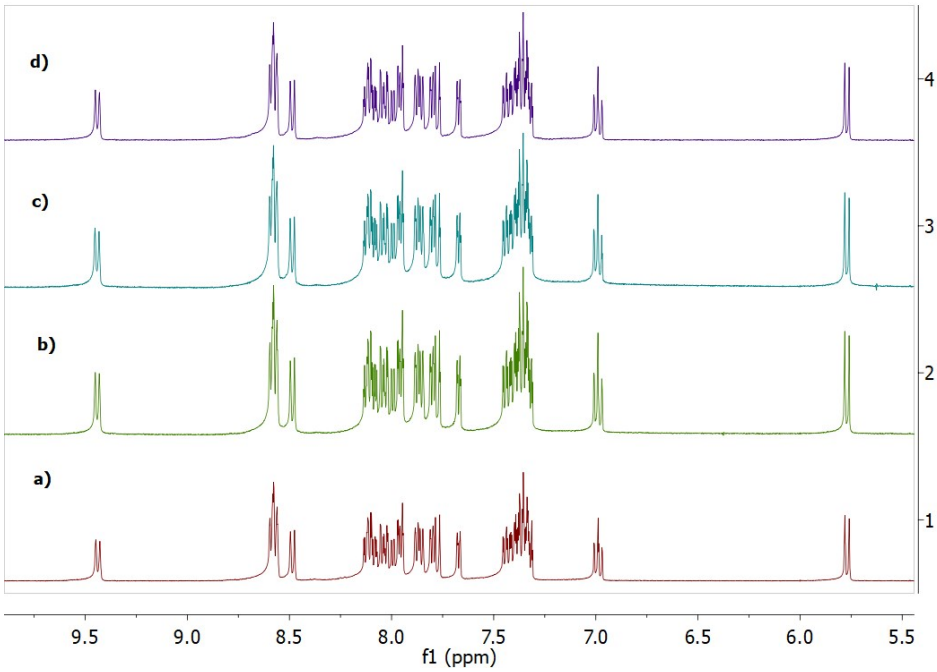

Figure SI9. Aromatic Area of ^{1}H NMR (400 MHz) spectra of **[Ru1]Cl_2** in CD_3CN ($1.4\cdot10^{-2}$ M) at 25 °C after irradiation with Blue LED light (λ=460 nm): a) t= 0, b) t= 2 h, c) t= 6 h and d) t= 24 h.

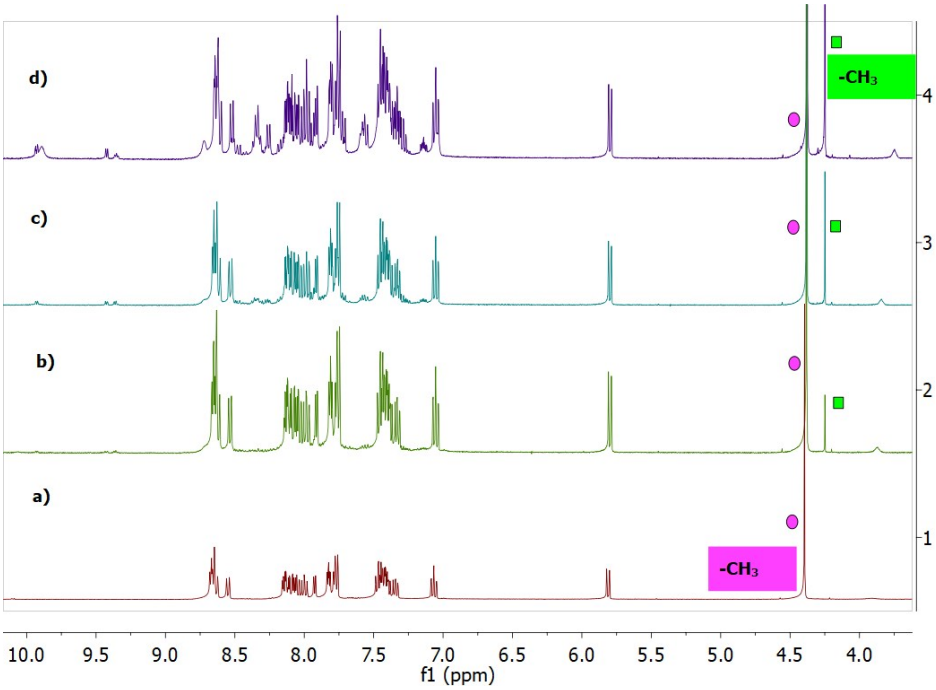

Figure SI10. Aromatic Area of ^{1}H NMR (400 MHz) spectra of **[Ru2]Cl$_2$** (pink circles) in CD_3CN ($1.4\cdot10^{-2}$ M) at 25 °C after irradiation with Blue LED light (λ=460 nm): a) t= 0, b) t= 2 h, c) t= 6 h and d) t= 24 h. (green squares = **L2**)

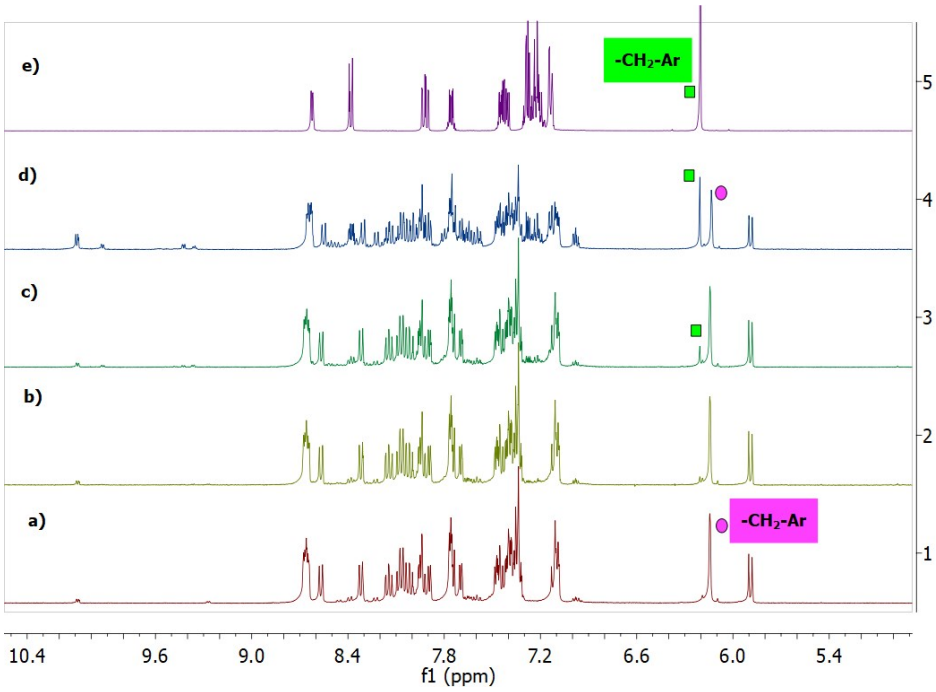

Figure SI11. Aromatic Area of ^{1}H NMR (400 MHz) spectra of **[Ru3]Cl$_2$** (pink circles) in CD_3CN ($1.4\cdot10^{-2}$ M) at 25 °C after irradiation with Blue LED light (λ=460 nm): a) t= 0, b) t= 2 h, c) t= 6 h and d) t= 24 h, e) **L3** (green squares).

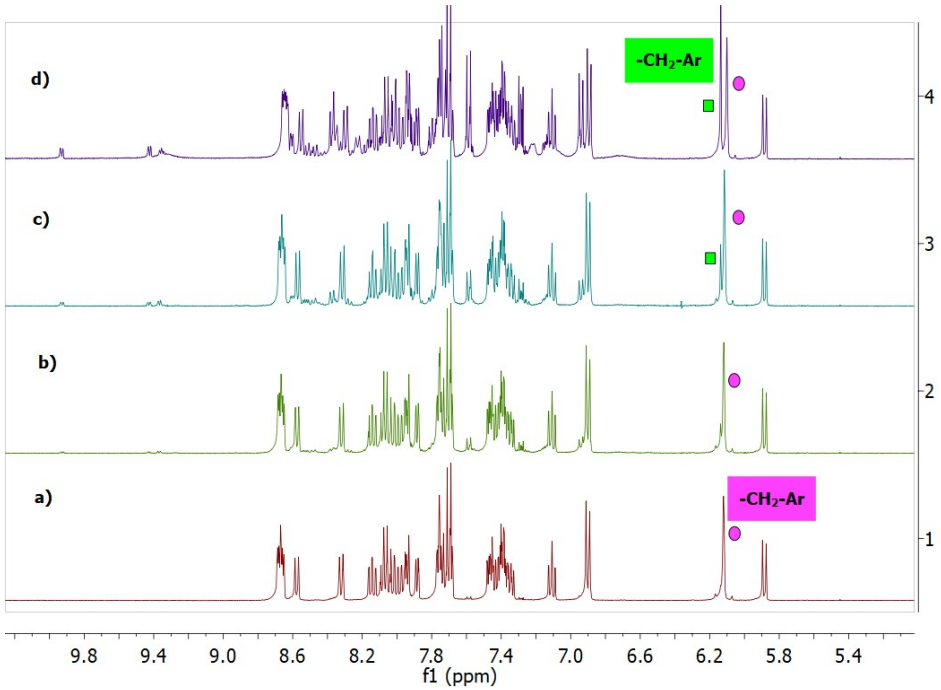

Figure SI12. Aromatic Area of ^{1}H NMR (400 MHz) spectra of **[Ru4]Cl$_2$** (pink circle) in CD_3CN ($1.4 \cdot 10^{-2}$ M) at 25 °C after irradiation with Blue LED light (λ=460 nm): a) t= 0, b) t= 2 h, c) t= 6 h and d) t= 24 h. (green squares = **L4**).

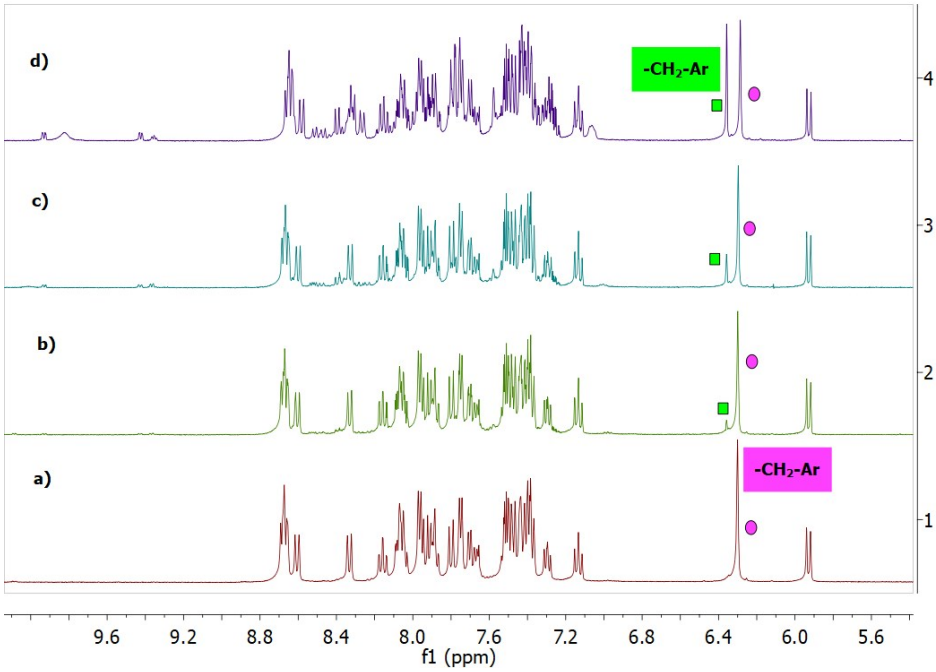

Figure SI13. Aromatic Area of ^{1}H NMR (400 MHz) spectra of **[Ru5]Cl$_2$** (pink circle) in CD_3CN ($1.4 \cdot 10^{-2}$ M) at 25 °C after irradiation with Blue LED light (λ=460 nm): a) t= 0, b) t= 2 h, c) t= 6 h and d) t= 24 h (green squares = **L5**).

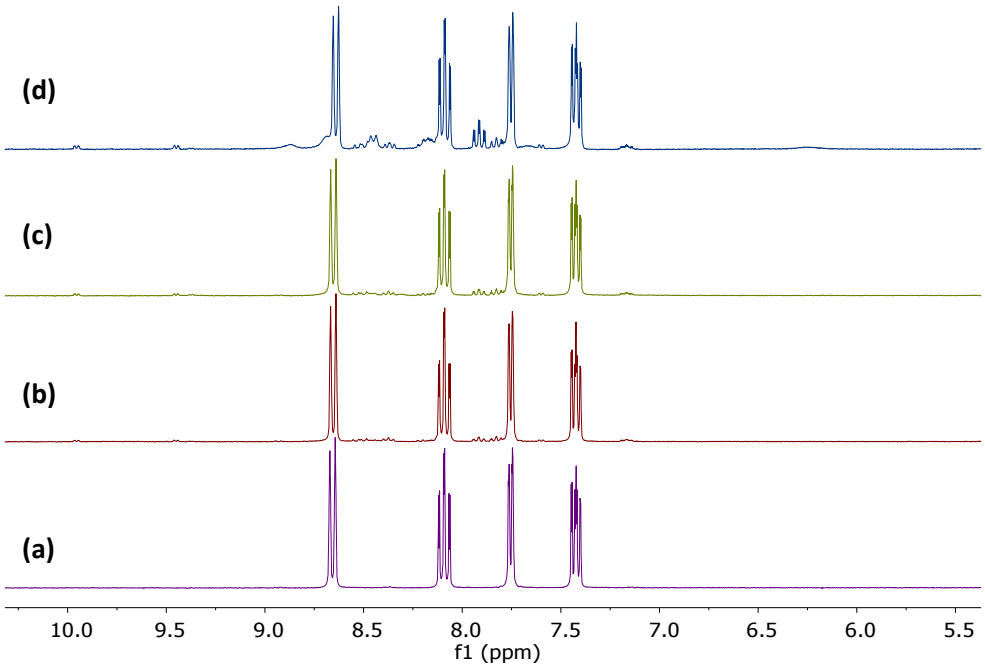

Figure SI14. Aromatic Area of ^{1}H NMR (400 MHz) spectra of **[1]Cl$_2$** in CD_3CN ($1.4 \cdot 10^{-2}$ M) at 25 °C after irradiation with Blue LED light (λ=460 nm): a) t= 0, b) t= 4 h, c) t= 6 h, d) t= 24 h.

5. Theoretical Calculations

Density functional theory (DFT) calculations were carried out with the D.01 revision of the Gaussian 09 package,[6] using the Becke's three-parameter B3LYP exchange-correlation functional,[7,8] together with the 6-31G(d,p) basis set for H, C, N, O, F, and S,[9,10] and the "double-zeta" quality LANL2DZ basis set for the Ru element.[11] The geometries of the singlet ground state (S_0) and the lowest-energy triplet state (T1) were fully optimized without imposing any symmetry restriction. The geometries of the triplet states were calculated at the spin-unrestricted UB3LYP level with a spin multiplicity of 3. All the calculations were performed in the presence of the solvent (acetonitrile). Solvent effects were considered within the self-consistent reaction field (SCRF) theory using the SMD keyword that performs a polarized continuum model (IEFPCM)[11] calculation using the solvatation model of Thrular et al.[12] Time-dependent DFT (TD-DFT) calculations of the lowest-lying 15 singlets and triplets were performed in the presence of the solvent at the minimum-energy geometry optimized for the ground state (S_0).

[6] M. J. Frisch, G. W. Trucks, H. B. Schlegel, G. E. Scuseria, M. A. Robb, J. R. Cheeseman, G. Scalmani, V. Barone, B. Mennucci, G. A. Petersson, H. Nakatsuji, M. Caricato, X. Li, H. P. Hratchian, A. F. Izmaylov, J. Bloino, G. Zheng, J. L. Sonnenberg, M. Hada, M. Ehara, K. Toyota, R. Fukuda, J. Hasegawa, M. Ishida, T. Nakajima, Y. Honda, O. Kitao, H. Nakai, T. Vreven, J. A. Montgomery, Jr., J. E. Peralta, F. Ogliaro, M. Bearpark, J. J. Heyd, E. Brothers, K. N. Kudin, V. N. Staroverov, R. Kobayashi, J. Normand, K. Raghavachari, A. Rendell, J. C. Burant, S. S. Iyengar, J. Tomasi, M. Cossi, N. Rega, J. M. Millam, M. Klene, J. E. Knox, J. B. Cross, V. Bakken, C. Adamo, J. Jaramillo, R. Gomperts, R. E. Stratmann, O. Yazyev, A. J. Austin, R. Cammi, C. Pomelli, J. W. Ochterski, R. L. Martin, K. Morokuma, V. G. Zakrzewski, G. A. Voth, P. Salvador, J. J. Dannenberg, S. Dapprich, A. D. Daniels, Ö. Farkas, J. B. Foresman, J. V. Ortiz, J. Cioslowski, and D. J. Fox, *Gaussian 09* (Gaussian, Inc., Wallingford CT, 2009)

[7] A. D. Becke, *J. Chem. Phys.* **1993**, *98*, 5648–5652

[8] C. Lee, W. Yang, R. G. Parr, *Phys. Rev. B* **1988**, *37*, 785–789.

[9] M. M. Francl, W. J. Pietro, W. J. Hehre, J. S. Binkley, M. S. Gordon, D. J. DeFrees, J. A. Pople, *J. Chem. Phys.* **1982**, *77*, 3654–3665

[10] P. C. Hariharan, J. A. Pople, *Theor. Chim. Acta* **1973**, *28*, 213–222

[11] G. Scalmani, M. J. Frisch, *J. Chem. Phys.* **2010**, *132*, 114110.

[12] A. V Marenich, C. J. Cramer, D. G. Truhlar, *J. Phys. Chem. B* **2009**, *113*, 6378–6396.

Table SI2. Lowest triplet excited states calculated at the TD-DFT B3LYP/(6-31G**+LANL2DZ) level for complexes **[Ru1]$^{2+}$** to **[Ru3]$^{2+}$** in acetonitrile solution. Vertical excitation energies (E), dominant monoexcitations with contributions (within parentheses) greater than 15%, nature of the electronic transition and description of the excited state are summarized. H and L denote HOMO and LUMO, respectively.

Compound	State	E (eV; nm) / *f*	Monoexcitations	Nature	Description
[Ru1]Cl_2	S_1	2.64; 469 / 0.0007	H→L (52)	$d_\pi(Ru) + \pi_{L1} \rightarrow \pi^*_{bpy} + \pi^*_{L1}$	^{1}MLCT/^{1}LLCT/^{1}LC
			H→ L+2 (48)	$d_\pi(Ru) + \pi_{L1} \rightarrow \pi^*_{bpy} + \pi^*_{L1}$	^{1}MLCT/^{1}LLCT/^{1}LC
	S_2	2.67; 464 / 0.0022	H→ L (28)	$d_\pi(Ru) + \pi_{L1} \rightarrow \pi^*_{bpy} + \pi^*_{L1}$	^{1}MLCT/^{1}LLCT/^{1}LC
			H→ L+1 (47)	$d_\pi(Ru) + \pi_{L1} \rightarrow \pi^*_{bpy} + \pi^*_{L1}$	^{1}MLCT/^{1}LLCT/^{1}LC
			H→ L+2 (20)	$d_\pi(Ru) + \pi_{L1} \rightarrow \pi^*_{bpy} + \pi^*_{L1}$	^{1}MLCT/^{1}LLCT/^{1}LC
	S_3	2.70; 459 / 0.0034	H→ L (20)	$d_\pi(Ru) + \pi_{L1} \rightarrow \pi^*_{bpy} + \pi^*_{L1}$	^{1}MLCT/^{1}LLCT/^{1}LC
			H→ L+1 (44)	$d_\pi(Ru) + \pi_{L1} \rightarrow \pi^*_{bpy} + \pi^*_{L1}$	^{1}MLCT/^{1}LLCT/^{1}LC
			H→ L+2 (31)	$d_\pi(Ru) + \pi_{L1} \rightarrow \pi^*_{bpy} + \pi^*_{L1}$	^{1}MLCT/^{1}LLCT/^{1}LC
	T_1	2.43; 510 / ----	H→ L+1 (52)	$d_\pi(Ru) + \pi_{L1} \rightarrow \pi^*_{bpy} + \pi^*_{L1}$	^{3}MLCT/^{3}LLCT/^{3}LC
			H→ L+2 (34)	$d_\pi(Ru) + \pi_{L1} \rightarrow \pi^*_{bpy} + \pi^*_{L1}$	^{3}MLCT/^{3}LLCT/^{3}LC
	T_2	2.50; 497 / ----	H→ L+1 (44)	$d_\pi(Ru) + \pi_{L1} \rightarrow \pi^*_{bpy} + \pi^*_{L1}$	^{3}MLCT/^{3}LLCT/^{3}LC
			H→ L+2 (50)	$d_\pi(Ru) + \pi_{L1} \rightarrow \pi^*_{bpy} + \pi^*_{L1}$	^{3}MLCT/^{3}LLCT/^{3}LC
	T_3	2.52; 491 / ----	H→ L (72)	$d_\pi(Ru) + \pi_{Lx} \rightarrow \pi^*_{bpy} + \pi^*_{L1}$	^{3}MLCT/^{3}LLCT/^{3}LC
[Ru2]Cl_2	S_1	2.61; 474 /0.0007	H→L (48)	$d_\pi(Ru) + \pi_{L2} \rightarrow \pi^*_{bpy} + \pi^*_{L2}$	^{1}MLCT/^{1}LLCT/^{1}LC
			H→ L+2 (48)	$d_\pi(Ru) + \pi_{L2} \rightarrow \pi^*_{bpy} + \pi^*_{L2}$	^{1}MLCT/^{1}LLCT/^{1}LC
	S_2	2.65; 469 /0.0023	H→ L (21)	$d_\pi(Ru) + \pi_{L2} \rightarrow \pi^*_{bpy} + \pi^*_{L2}$	^{1}MLCT/^{1}LLCT/^{1}LC
			H→ L+1 (64)	$d_\pi(Ru) + \pi_{L2} \rightarrow \pi^*_{bpy} + \pi^*_{L2}$	^{1}MLCT/^{1}LLCT/^{1}LC
	S_3	2.68; 463 /0.0049	H→ L (30)	$d_\pi(Ru) + \pi_{L2} \rightarrow \pi^*_{bpy} + \pi^*_{L2}$	^{1}MLCT/^{1}LLCT/^{1}LC
			H→ L+1 (22)	$d_\pi(Ru) + \pi_{L2} \rightarrow \pi^*_{bpy} + \pi^*_{L2}$	^{1}MLCT/^{1}LLCT/^{1}LC
			H→ L+2 (41)	$d_\pi(Ru) + \pi_{L2} \rightarrow \pi^*_{bpy} + \pi^*_{L2}$	^{1}MLCT/^{1}LLCT/^{1}LC
	T_1	2.39; 518 / ----	H→ L+1 (52)	$d_\pi(Ru) + \pi_{L2} \rightarrow \pi^*_{bpy} + \pi^*_{L2}$	^{3}MLCT/^{3}LLCT/^{3}LC
			H→ L+2 (43)	$d_\pi(Ru) + \pi_{L2} \rightarrow \pi^*_{bpy} + \pi^*_{L2}$	^{3}MLCT/^{3}LLCT/^{3}LC
	T_2	2.47; 502 / ----	H→ L+1 (47)	$d_\pi(Ru) + \pi_{L2} \rightarrow \pi^*_{bpy} + \pi^*_{L2}$	^{3}MLCT/^{3}LLCT/^{3}LC
			H→ L+2 (47)	$d_\pi(Ru) + \pi_{L2} \rightarrow \pi^*_{bpy} + \pi^*_{L2}$	^{3}MLCT/^{3}LLCT/^{3}LC
	T_3	2.51; 494 / ----	H→ L (79)	$d_\pi(Ru) + \pi_{L2} \rightarrow \pi^*_{bpy} + \pi^*_{L2}$	^{3}MLCT/^{3}LLCT/^{3}LC
[Ru3]Cl_2	S_1	2.62;473 / 0.0011	H→L (24)	$d_\pi(Ru) + \pi_{L3} \rightarrow \pi^*_{bpy} + \pi^*_{L3}$	^{1}MLCT/^{1}LLCT/^{1}LC
			H→ L+1 (29)	$d_\pi(Ru) + \pi_{L3} \rightarrow \pi^*_{bpy} + \pi^*_{L3}$	^{1}MLCT/^{1}LLCT/^{1}LC
			H→ L+2 (44)	$d_\pi(Ru) + \pi_{L3} \rightarrow \pi^*_{bpy}$	^{1}MLCT/^{1}LLCT
	S_2	2.65; 469 / 0.0011	H→ L+1 (60)	$d_\pi(Ru) + \pi_{L3} \rightarrow \pi^*_{bpy} + \pi^*_{L3}$	^{1}MLCT/^{1}LLCT/^{1}LC
			H→ L+2 (27)	$d_\pi(Ru) + \pi_{L3} \rightarrow \pi^*_{bpy}$	^{1}MLCT/^{1}LLCT
	S_3	2.67; 465 / 0.0061	H→ L (71)	$d_\pi(Ru) + \pi_{L3} \rightarrow \pi^*_{bpy} + \pi^*_{L3}$	^{1}MLCT/^{1}LLCT/^{1}LC
			H→ L+2 (27)	$d_\pi(Ru) + \pi_{L3} \rightarrow \pi^*_{bpy}$	^{1}MLCT/^{1}LLCT
	T_1	2.37; 522 / ----	H→ L+1 (85)	$d_\pi(Ru) + \pi_{L3} \rightarrow \pi^*_{bpy} + \pi^*_{L3}$	^{3}MLCT/^{3}LLCT/^{3}LC
	T_2	2.48; 500 / ----	H→ L+2 (87)	$d_\pi(Ru) + \pi_{L3} \rightarrow \pi^*_{bpy}$	^{3}MLCT/^{3}LLCT
	T_3	2.52; 493 / ----	H→ L (71)	$d_\pi(Ru) + \pi_{L3} \rightarrow \pi^*_{bpy} + \pi^*_{L3}$	^{3}MLCT/^{3}LLCT/^{3}LC
[Ru(bpy)$_3$]Cl_2	S_1	2.72; 456 / 0.0000	H→L+1 (28)	$d_\pi(Ru) \rightarrow \pi^*_{bpy}$	^{1}MLCT
			H→L+2 (72)	$d_\pi(Ru) \rightarrow \pi^*_{bpy}$	
	S_2	2.72; 456 / 0.0001	H→L+1 (70)	$d_\pi(Ru) \rightarrow \pi^*_{bpy}$	^{1}MLCT
			H→L+2 (28)	$d_\pi(Ru) \rightarrow \pi^*_{bpy}$	
	S_3	2.72; 455 / 0.0013	H→L (100)	$d_\pi(Ru) \rightarrow \pi^*_{bpy}$	^{1}MLCT
	T_1	2.54; 488 / ----	H→L+1 (100)	$d_\pi(Ru) \rightarrow \pi^*_{bpy}$	^{3}MLCT
	T_2	2.54; 488 / ----	H→L+2 (100)	$d_\pi(Ru) \rightarrow \pi^*_{bpy}$	^{3}MLCT
	T_3	2.59; 479 / ----	H→L (95)	$d_\pi(Ru) \rightarrow \pi^*_{bpy}$	^{3}MLCT

Table SI3.- Topologies and energies (eV) of the MOs of three representative Ru(II)-complexes and **$[Ru(bpy)_3]Cl_2$**

	$[Ru1]Cl_2$	**$[Ru2]Cl_2$**	**$[Ru3]Cl_2$**	**$[Ru(bpy)_3]Cl_2$**
LUMO +2	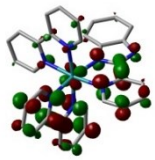 -2.45909413	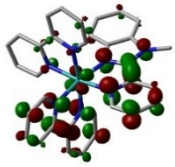 -2.45283551	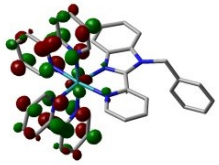 -2.4623595	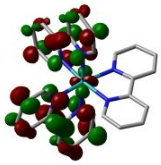 -2.47950268
LUMO +1	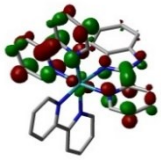 -2.46508064	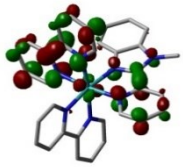 -2.46372007	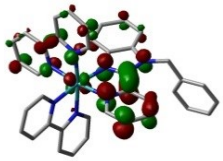 -2.49038724	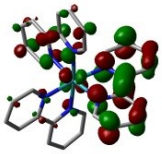 -2.4800469
LUMO	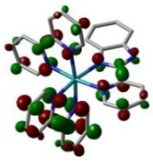 -2.5537898	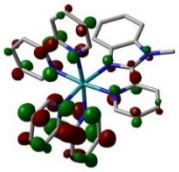 -2.54399369	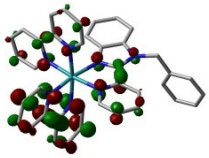 -2.54943597	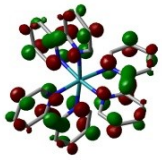 -2.57637526
HOMO	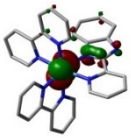 -6.03439984	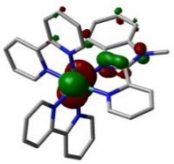 -5.996576	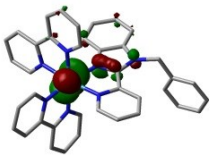 -6.01535186	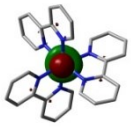 -6.13698682
HOMO -1	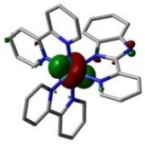 - 6.1949471	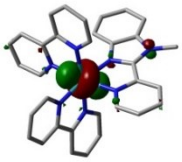 -6.17181741	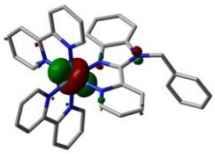 -6.19576344	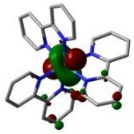 -6.30678595
HOMO -2	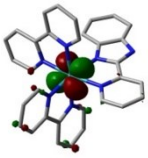 - 6.28392837	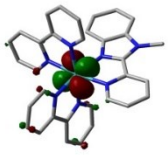 -6.26732942	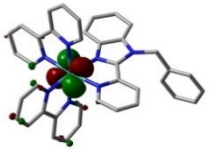 -6.27739764	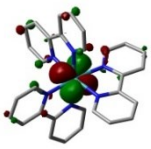 -6.30733017

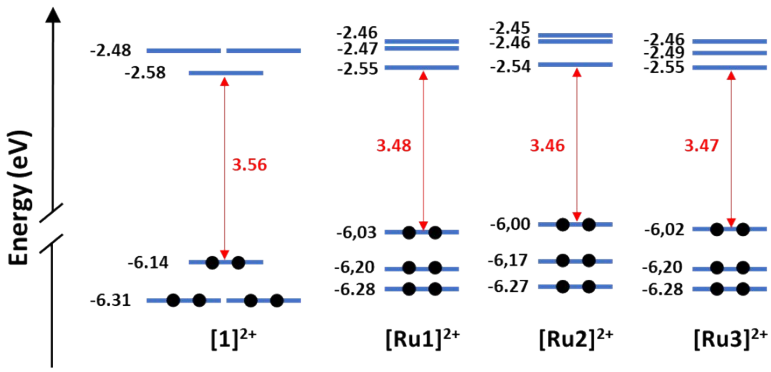

Fig. SI15.- Sketch representation showing the energies calculated for the frontier molecular orbitals of **[1]$^{2+}$** and **[Ru1]$^{2+}$**–**[Ru3]$^{2+}$**.

6. Determination of $^1O_2$ generation quantum yields

Singlet Oxygen quantum yields (ϕ_Δ^{PC}) were determined for selected Ru(II) photocatalysts (**PCs**) in acetonitrile according to a relative procedure adapted from the literature,[13] which is based on monitoring by UV-Vis spectroscopy the oxidation of 1,3-diphenylisobenzofuran (DPBF, yellow) to 1,2-dibenzoylbenzene (colorless) photosensitized by the Ru(II) derivatives.

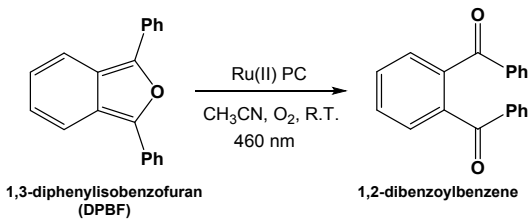

DPBF was selected as the $^1O_2$ scavenger due to its fast reaction with $^1O_2$. Air-equilibrated acetonitrile solutions containing DPBF were prepared (~$8\cdot10^{-5}$ M) in a cuvette and their absorbance adjusted to around 1.0 at 410 nm. Then, the photosensitizer (either Ru-**PC** or $[Ru(bpy)_3]Cl_2$, **[1]Cl$_2$**; 10^{-5} M, corresponding to absorbance around 0.2) was introduced in the cuvette. Low dye concentrations were used to minimize quenching of $^1O_2$ by the dyes. The mixture was irradiated with a blue LED strip (λ_{irr} = 460 nm) at room temperature for 1 second irradiation intervals during a total exposure period of 8 seconds and absorption UV-Vis spectra were recorded after every irradiation interval. The decrease in the absorption band at 410 nm was plotted *vs.* the irradiation time and the experimental data were fitted to a straight line. An acetonitrile solution of DPBF without the Ru(II) complex was examined to confirm its photostability under identical irradiation conditions (8 s). The ϕ_Δ^{PC} were calculated by a relative method using equation (1), and $[Ru(bpy)_3]Cl_2$ (**[1]Cl$_2$**) as the reference for $^1O_2$ photosensitization in acetonitrile (ϕ_Δ^S = 0.56).[14]

$$\phi_\Delta^{PC} = \phi_\Delta^S \times (S^{PC} \times F^S) / (S^S \times F^{PC}) \qquad \text{eq (1)}$$

[13] a) N. Adarsh, R. R. Avirah and D. Ramaiah, *Org. Lett.*, 2010, **12**, 5720–5723, b) P. Majumdar, X. Yuan, S. Li, B. Le Guennic, J. Ma, C. Zhang, D. Jacquemin and J. Zhao, *J. Mater. Chem. B*, 2014, **2**, 2838–2854, c) S. P.-Y. Li, C. T.-S. Lau, M.-W. Louie, Y.-W. Lam, S. H. Cheng and K. K.-W. Lo, *Biomaterials*, 2013, **34**, 7519–7532.
[14] Y. Lu, R. Conway-Kenny, J. Wang, X. Cui, J. Zhao and S. M. Draper, *Dalt. Trans.*, 2018, **47**, 8585–8589.

Where S, is the slope of a linear fit for the change in absorbance of DPBF (at 410 nm) with the irradiation time, and F, is the absorption correction factor, which is given by $F = 1-10^{-OD}$ (where OD is the optical density at the irradiation wavelength). The superscripts PC and S stand for the Ru(II) photocatalysts and the standard sensitizer, **[1]Cl$_2$**, respectively.

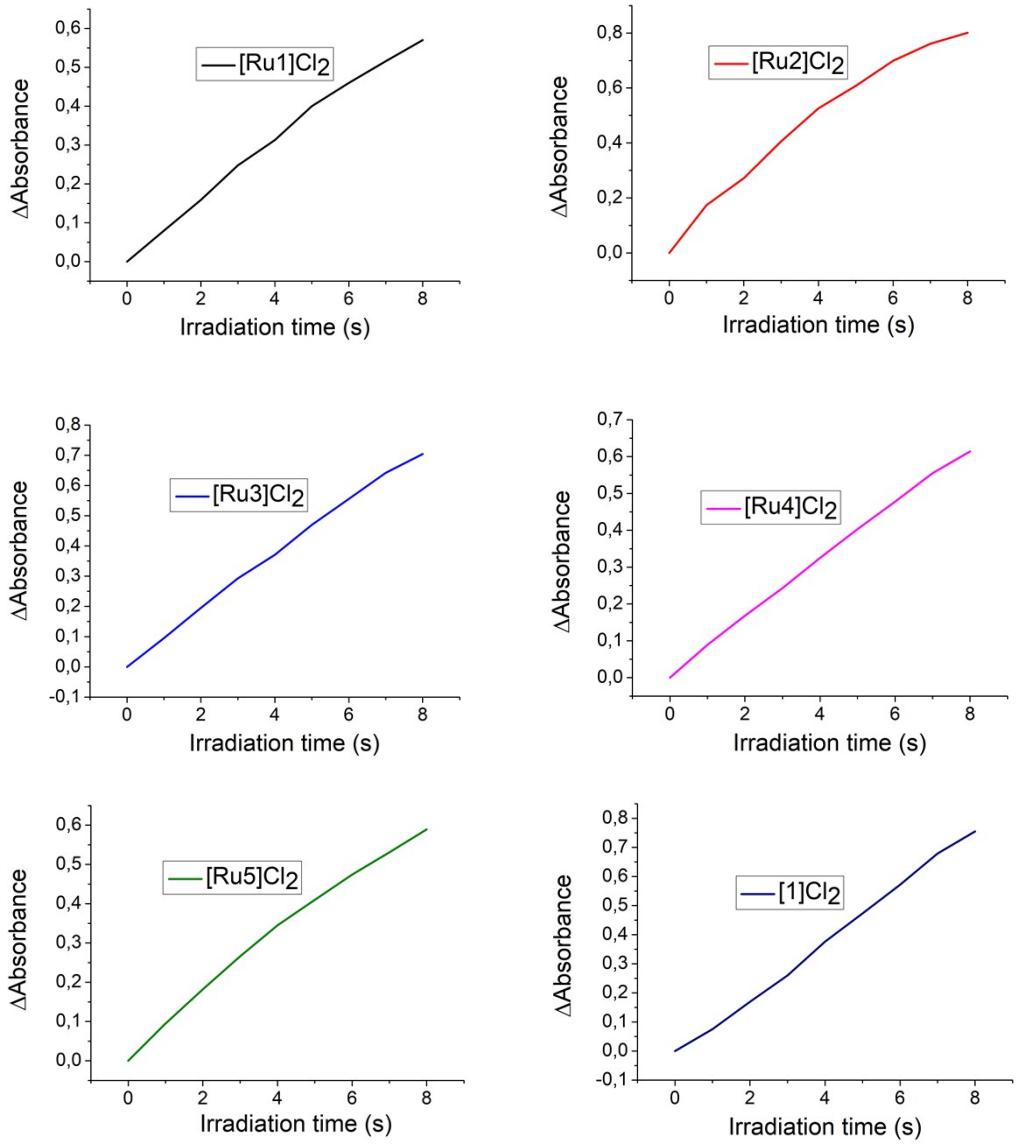

Figure SI16. Graphics obtained from the experimental data and used for the determination of $^1O_2$ generation quantum yields.

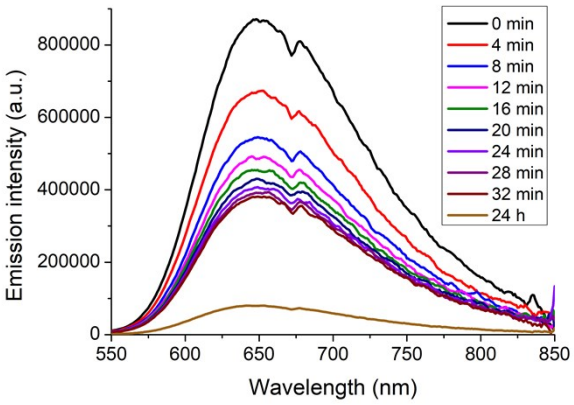

Figure SI17. Effect of the oxygen on the emission of **[Ru3]Cl_2** with the time.

7. Electrochemical measurements and individual CV of the Ru(II) complexes.

Electrochemical measurements were performed using a portable potentiostat/galvanostat PalmSens3 (PalmSens) equipment controlled by the software PSTrace4 Version 4.4.2. All experiments were carried out using a three-electrode cell with a glassy carbon-disc (diameter = 3 mm) as the working electrode, a platinum-wire as the auxiliary electrode, and a Ag/AgCl (MF-2052 BASi) reference electrode separated from the bulk solution by a Vycor™ frit. Oxygen was removed from the solution by bubbling argon for 5 minutes and keeping the current of argon along the whole experiment. The measurements were recorded for acetonitrile solutions of the Ru(II) complexes ($5\cdot\times 10^{-4}$ M) in the presence of [$n$$Bu_4$N][$PF_6$] (0.1 M) as the supporting electrolyte by cyclic voltammetry (CV) at a scan rate of 100 mV s^{-1} in a clockwise direction. Ferrocene was added at the end of all the experiments as the internal reference in order to refer the potentials to the redox pair ferrocenium/ferrocene (Fc^+/Fc) under the conditions of our experiments. The potential experimentally determined for the redox couple Fc^+/Fc was $E°_{1/2}$ = 0.443±0.005 V vs. Ag/AgCl. Therefore, the experimental redox potentials were calculated from the corresponding voltammograms as:

E° (vs AgCl/Ag) = (E_{ap} + E_{cp})/2, for reversible peaks where E_{ap} and E_{cp} stand for anodic and cathodic peak potentials, respectively. However, for irreversible peaks, the potentials were calculated as either the E_{ap} maximum or E_{cp} minimum.

E° (vs Fc^+/Fc) = E° (vs AgCl/Ag) – 0.443, for potential values reported in reference to the (Fc^+/Fc) redox couple.

E° (vs SCE) = E° (vs Fc^+/Fc) + 0.404, for potential values reported in reference to the saturated calomel electrode (SCE) and having into account that $E°_{1/2}$ (Fc^+/Fc) = 0.404 V *vs* SCE according to the literature.[15]

[15] Connelly, N. G.; Geiger, W. E. *Chem. Rev.* **1996**, *96*, 877–910

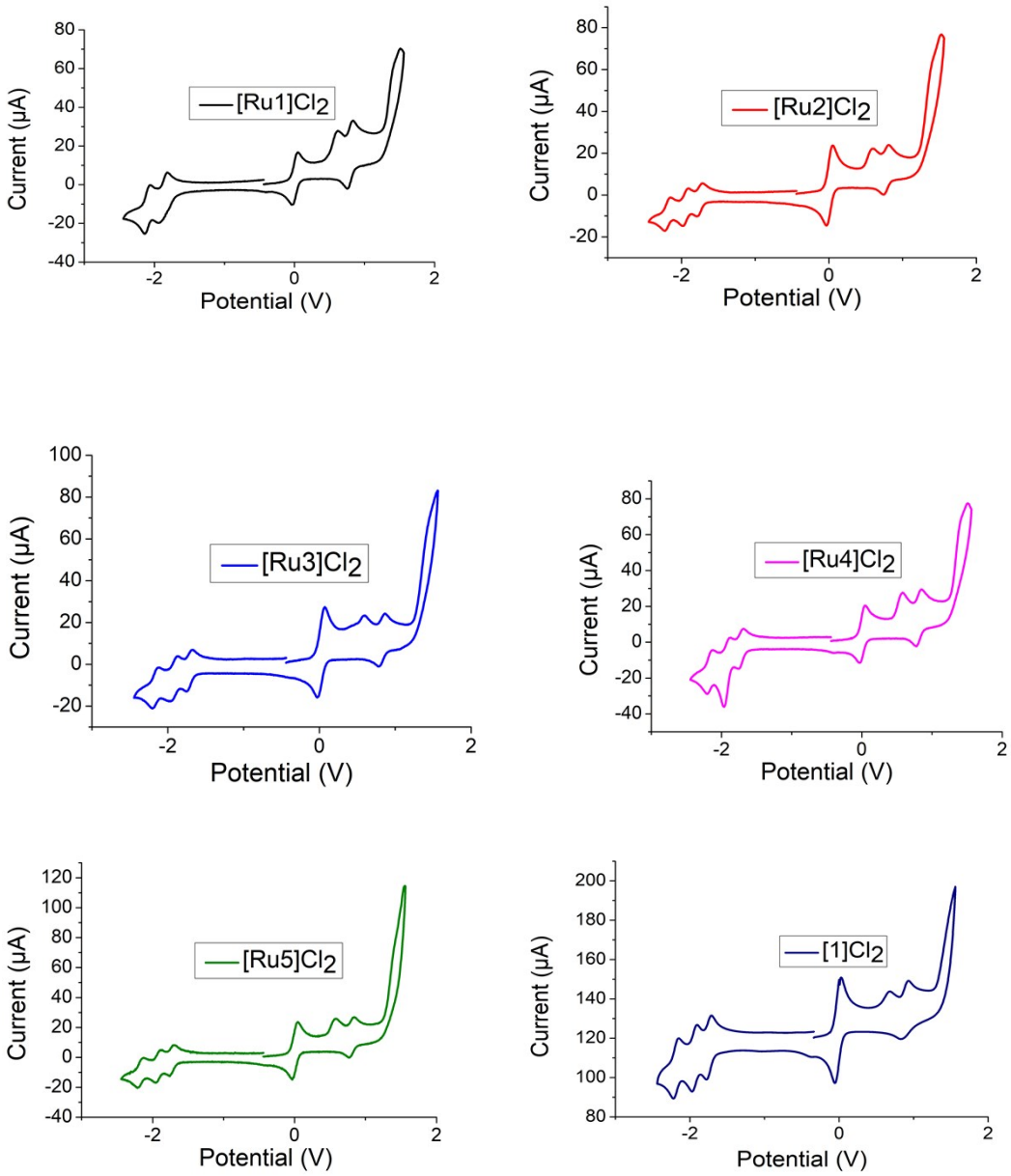

Figure SI18. Cyclic voltammograms of the ruthenium complexes.

Table SI4. Redox Potentials for the excited states versus Fc^+/Fc.[a]

Complex	$E°(Ru^{III}/Ru^{II})$	$E°(Ru^{II}/Ru^{I})$	$E°(Ru^{II*}/Ru^{II})$	$E°(Ru^{III}/Ru^{II*})$	$E°(Ru^{II*}/Ru^{I})$
[1]$(PF_6)_2$	+0.89	-1.73	2.00 eV (621 nm)	-1.11	+0.27
[Ru1]Cl_2	+0.80	-1.87	+1.91 (649 nm)	-1.11	+0.04
[Ru2]Cl_2	+0.78	-1.75	+1.92 (647 nm)	-1.14	+0.17
[Ru3]Cl_2	+0.83	-1.72	+1.89 (656 nm)	-1.06	+0.17
[Ru4]Cl_2	+0.81	-1.72	+1.89 (657 nm)	-1.08	+0.17
[Ru5]Cl_2	+0.80	-1.74	+1.91 (650 nm)	-1.11	+0.17

[a]All potential are given in volts versus Fc+/Fc. $E°(Ru^{III}/Ru^{II*}) = E°(Ru^{III}/Ru^{II}) - E°(Ru^{II*}/Ru^{II})$ and $E°(Ru^{II*}/Ru^{I}) = E°(Ru^{II}/Ru^{I}) + E°(Ru^{II*}/Ru^{II})$.

8.- Procedure for the photocatalytic oxidation of amines

In a septum-capped test tube the amine (5 μmol in solution of CH_3CN), the PC (Photocatalyst = 0.05 or 0.005 μmol in solution of CH_3CN), and additional CH_3CN to provide the desired final concentration of substrate (10 mM in 0.5 mL), were added. The system was purged with O_2 or N_2 until atmosphere saturation and irradiated with Blue LED light (λ= 460 nm, 24W) at room temperature during the required time. Then, an aliquot (100 μL) of the reaction mixture was diluted in CD_3CN (400 μL) and the mixture was analysed by ^1H NMR to determine the conversion. The yield values for the imines were calculated from the integration of the peaks assigned to the methylene groups of both the imine product (*e.g.*: doublet at 4.75 ppm for Ph-C**H$_2$**-N=CH-Ph, **2a**) and the benzyl amine used as reactant (*e.g.*: singlet at 3.78 ppm for Ph-C**H$_2$**-NH_2, **1a**).

Table SI6. Substrate Scope for the photooxidation of primary and secondary amines [a]

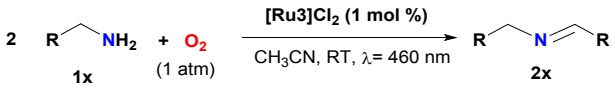

Entry	Substrate	Product	Yield (%)[Time (min)]
1	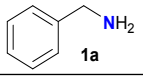 1a	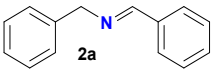 2a	98 [15] **>99 [30]**
2	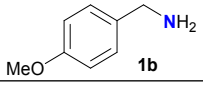 1b	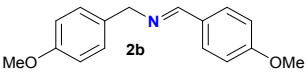 2b	**99 [30]**
3	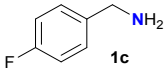 1c	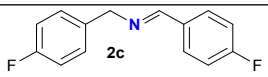 2c	86 [30] **>99 [60]**
4	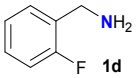 1d	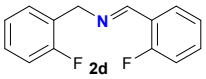 2d	87 [30] 95 [60] **>99 [90]**
5	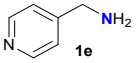 1e	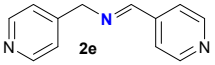 2e	**>99 [30]**
6	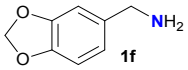 1f	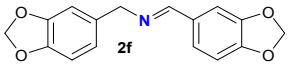 2f	62 [30] 89 [60] **>99 [90]**
7	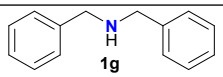 1g	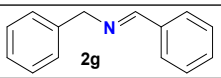 2g	**>99 [30]**
8	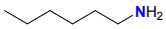 1h	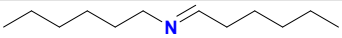 2h	**>99 [30]**
9	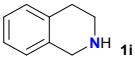 1i	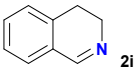 2i	**>99 [30]**
10	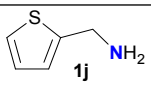 1j	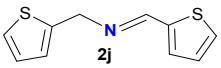 2j	94 [30] **>99 [60]**
11	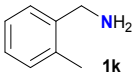 1k	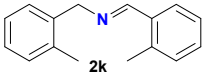 2k	**>99 [30]**

[a]Reaction Conditions: amine (10 mM), **[Ru3]Cl$_2$** (1 mol %), acetonitrile (0.5 mL), O_2 (balloon, 1 atm), blue LED light (λ= 460 nm), room temperature for the above-mentioned time. The yields were experimentally determined from ^1H NMR integration of the corresponding reaction crudes (see Supporting information). Reactions time between brackets.

9.- General One-pot procedure of photocatalyzed oxidative cyanation of amines

In a septum-capped glass test tube the amine **1a** (5 μmol in solution of CH_3CN), the **PC** (Photocatalyst = 0.05 μmol in solution of CH_3CN), TMSCN (10 μmol in solution of CH_3CN, 2 equiv.) and additional CH_3CN to provide the desired final concentration of substrate (10 mM in 0.5 mL) were placed. The system was purged with O_2 until atmosphere saturation and stirred under irradiation with Blue LED light (λ= 460 nm, 24W) at room temperature during the required time for the formation of the imine (30 min) and then under ambient light during the additional time required for the formation of the α-amino nitrile (5 h and a half for **1a**). Then, an aliquot (100 μL) of the reaction mixture was diluted in CD_3CN (400 μL) and the mixture was analysed by ^1H NMR to determine the yield of **3a**. The yield values for the α-amino nitriles were calculated from the integration of the peaks assigned to the methylene group of the α-amino nitrile product (e.g.: multiplet at 3.85 ppm for Ph-C**H_2**-NH-CH(CN)-Ph, **3a**) and the methylene group of the imine (*e.g.*: doublet at 4.75 ppm for Ph-**CH_2**-N=CH-Ph, **2a**).

For the isolation of the α-amino nitrile products the procedure was adapted according to the following amounts:

In a septum-capped glass test tube the amine **1a** (100 μmol in solution of CH_3CN), the **PC** (Photocatalyst = 1 μmol in solution of CH_3CN), TMSCN (200 μmol in solution of CH_3CN, 2 equiv.) and additional CH_3CN to provide the desired final concentration of substrate (20 mM in 5 mL) were placed. The system was purged with O_2 until atmosphere saturation and stirred under irradiation with Blue LED light (λ= 460 nm, 24W) at room temperature during the required time for the formation of the imine (30 min) and then under ambient light during the additional time required for the formation of the α-amino nitrile (5 h and a half for **1a**). Then, an aliquot (100 μL) of the reaction mixture was diluted in CD_3CN (400 μL) and the mixture was analysed by ^1H NMR to determine the yield of **3a**. The yield values for the α-amino nitriles were calculated from the integration of the peaks assigned to the methylene group of the α-amino nitrile product (*e.g.*: multiplet at 3.85 ppm for Ph-C**H_2**-NH-CH(CN)-Ph, **3a**) and the methylene group of the imine (*e.g.*: doublet at 4.75 ppm for Ph-**CH_2**-N=CH-Ph, **2a**). The products were isolated filtering the crude solution through a silica pad, using acetonitrile like mobile phase and at the end two millilitres of dichloromethane to assure the complete filtration of the product of interest. Then the products were dried under vacuum to constant weight. The ^1H NMR was recorded in $CDCl_3$.

10- Screening of different cyanide reagents with [Ru3]Cl_2 as PC.

Table SI5.

Substrate	Catalyst (mol %)	Solvent	Cyanide	Time (irradiation+stirring)	Conversion (%)
1a	1	AcCN:H_2O (98:2)	2 (KCN)	0,5 + 5,5	**1a**-71 **2a** -7 **3a**-22
	1	AcCN:H_2O (98:2)	2 ($K_3Fe(CN)_6$	0,5 + 5,5	**2a** -100
	1	AcCN:H_2O (98:2)	2 ($K_4Fe(CN)_6$ $3H_2O$	0,5 + 5,5	**1a**-75 **2a** -25

11.- ^{1}H NMR spectra and characterization of the crude and isolated α-amino nitriles

3a: 2-(benzylamino)-2-phenylacetonitrile

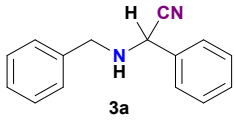

3a

^{1}H NMR of crude **3a (400 MHz, CD_3CN, 25 °C):** δ 7.58 – 7.53 (m, 2H), 7.46 – 7.28 (m, 8H), 4.77 (d, $^3J_{H-H}$ = 9.38 Hz, 1H, -CH(CN)), 3.91 (dd, $^2J_{H-H}$ = 13.5 Hz, $^3J_{H-H}$= 6.94 Hz, 1H, -CH_2) 3.82 (dd, $^2J_{H-H}$ = 13.5 Hz, $^3J_{H-H}$= 6.94 Hz,, 1H, -CH_2) ppm. **^{1}H NMR** of isolated **3a (400 MHz, $CDCl_3$, 25 °C)** δ 7.58 – 7.53 (m, 2H), 7.46 – 7.28 (m, 8H), 4.77 (s, 1H), 4.06 (d, $^2J_{H-H}$ = 12.9 Hz, 1H, -CH_2), 3.95 (d, $^2J_{H-H}$ = 12.9 Hz, 1H, -CH_2),ppm. **HR ESI+ MS (CH_2Cl_2):** [M+H$^+$] calcd. for $[C_{15}H_{15}N_2]^+$ 223.1235, found 223.1234. Note: In CD_3CN the diastereotopic -CH_2- and the -CH(CN)- protons are coupled to the NH, whereas in $CDCl_3$ these couplings are not observed.

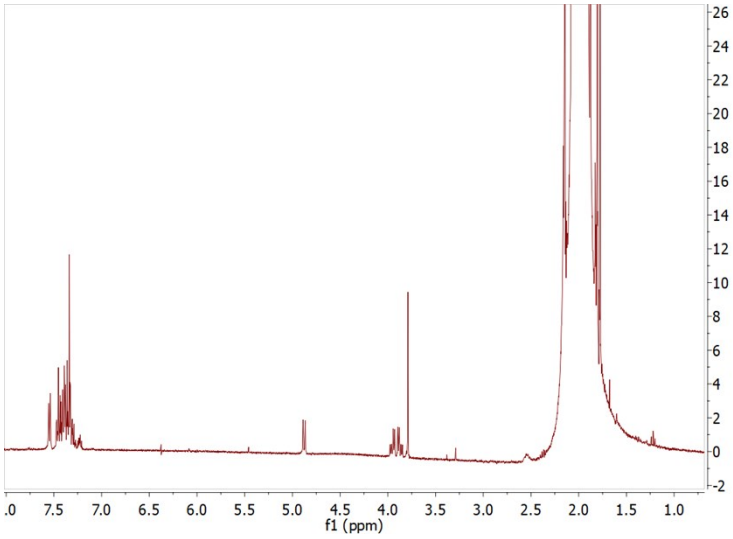

Figure SI19. ^{1}H NMR spectrum in CD_3CN for the crude **3a** of the photocatalytic oxidative cyanation of amine (**1a,** 20 mM) in the presence of the photocatalyst **[Ru3]Cl_2** (1 mol%) in CH_3CN under O_2 and blue LED irradiation (λ_{exc} = 460 nm) at room temperature.

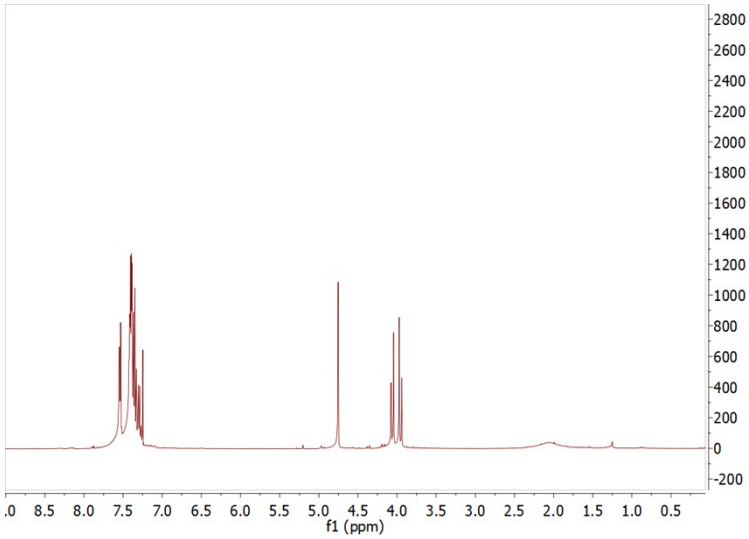

Figure SI20. ^{1}H NMR spectrum in $CDCl_3$ for the isolated cyanide **3a** of the photocatalytic oxidative cyanation of amine (**1a,** 20 mM) in the presence of the photocatalyst **[Ru3]Cl_2** (1 mol%) in CH_3CN under O_2 and blue LED irradiation (λ_{exc} = 460 nm) at room temperature.

3b: 2-((4-methoxybenzyl)amino)-2-(4-methoxyphenyl)acetonitrile

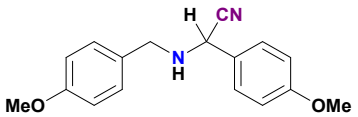

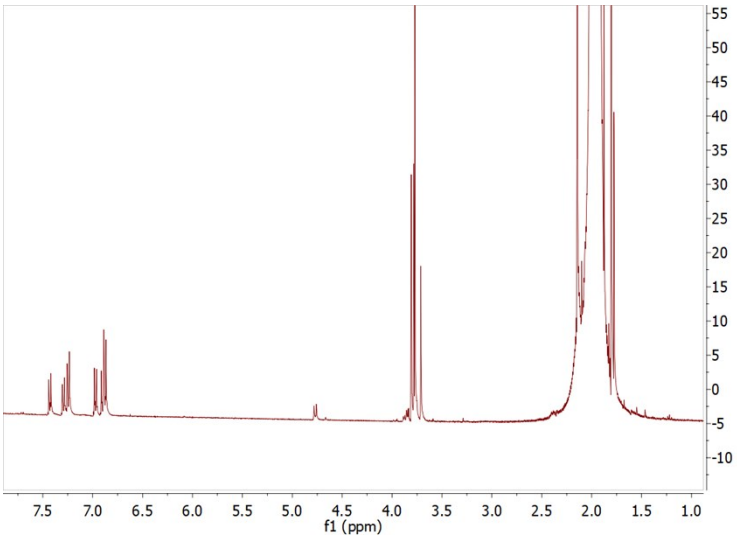

Figure SI21. ^{1}H NMR spectrum in CD_3CN for the crude **3b** of the photocatalytic oxidative cyanation of amine (**1b,** 20 mM) in the presence of the photocatalyst **[Ru3]Cl$_2$** (1 mol%) in CH_3CN under O_2 and blue LED irradiation (λ_{exc} = 460 nm) at room temperature.

3c: 2-((4-fluorobenzyl)amino)-2-(4-fluorophenyl)acetonitrile

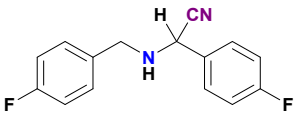

3c

^{1}H NMR (isolated) (400 MHz, CDCl$_3$, 25 °C) δ 7.59 – 7.47 (m, 2H), 7.40 – 7.31 (m, 2H), 7.21 – 7.09 (m, 2H), 7.09 – 6.99 (m, 2H), 4.83 (d, J = 9.7 Hz, 1H), 4.01 (d, J= 13.05 Hz, 1H, CH_2), 3.90 (d, J= 13.05 Hz, 1H, CH_2) ppm. **HR ESI+ MS (CH$_2$Cl$_2$, 4:1):** [M+H$^+$] calcd. for $[C_{15}H_{13}F_2N_2]^+$ 259.1047, found 259.1047

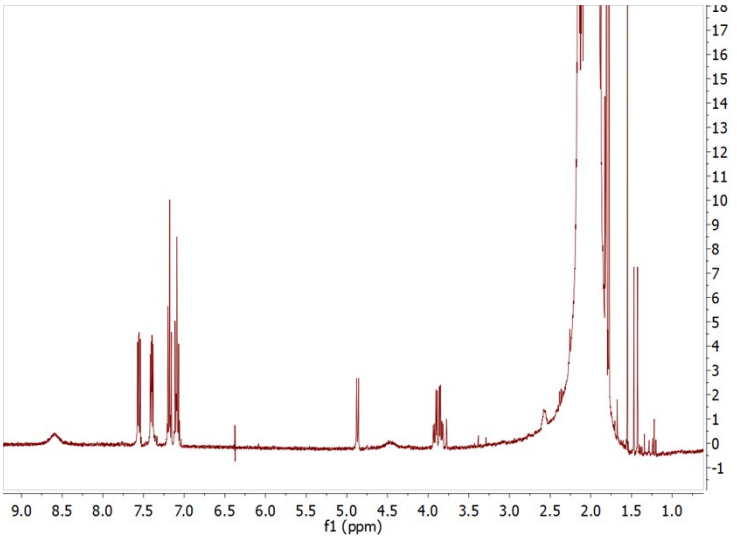

Figure SI22. ^{1}H NMR spectrum in CD_3CN for the crude **3c** of the photocatalytic oxidative cyanation of amine (**1c,** 20 mM) in the presence of the photocatalyst **[Ru3]Cl$_2$** (1 mol%) in CH_3CN under O_2 and blue LED irradiation (λ_{exc} = 460 nm) at room temperature.

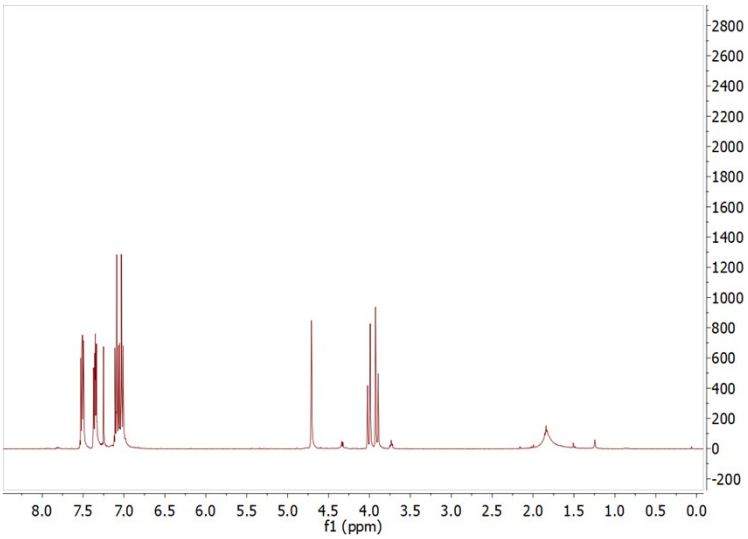

Figure SI23. ^{1}H NMR spectrum in $CDCl_3$ for the isolate cyanide **3c** of the photocatalytic oxidative cyanation of amine (**1c,** 20 mM) in the presence of the photocatalyst **[Ru3]Cl$_2$** (1 mol%) in CH_3CN under O_2 and blue LED irradiation (λ_{exc} = 460 nm) at room temperature.

3f: 2-(benzo[d][1,3]dioxol-5-yl)-2-((benzo[d][1,3]dioxol-5-ylmethyl)amino)acetonitrile

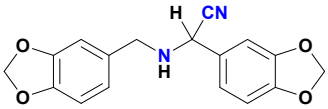

3f

^{1}H NMR (isolated) (400 MHz, $CDCl_3$, 25 °C) δ 6.99 (m, 1H), 6.80 (m, 3H), 5.95 (m, 3H), 4.64 (s, 1H), 3.93 (d, J= 13.3 Hz, 1H, CH_2), 3.82 (d, J= 13.3 Hz, 1H, CH_2), 1.54 (m, 4H) ppm.

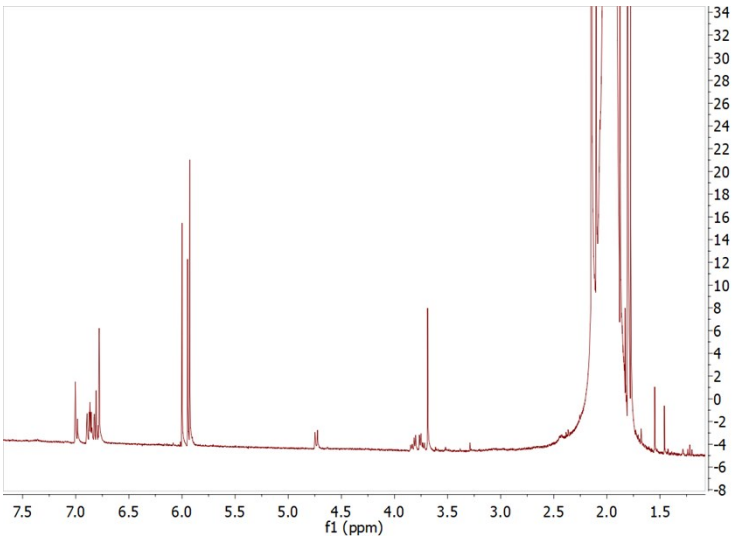

Figure SI24. ^{1}H NMR spectrum in CD_3CN for the crude **3f** of the photocatalytic oxidative cyanation of amine (**1f,** 20 mM) in the presence of the photocatalyst **[Ru3]Cl$_2$** (1 mol%) in CH_3CN under O_2 and blue LED irradiation (λ_{exc} = 460 nm) at room temperature.

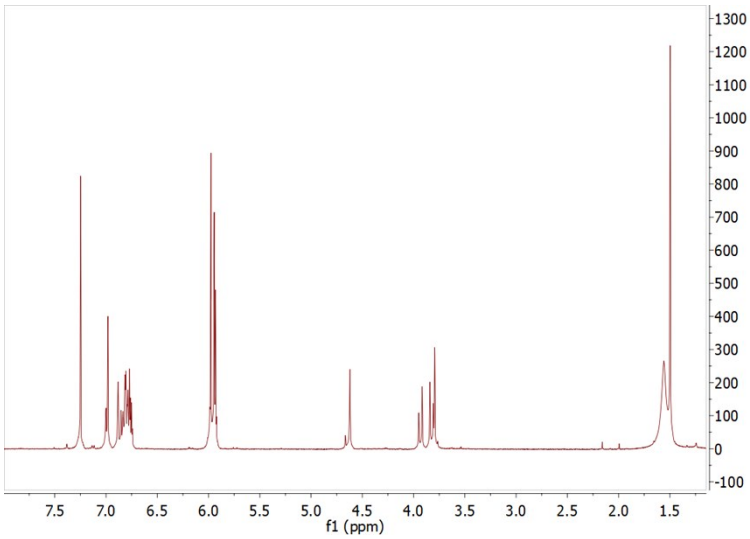

Figure SI25. ^{1}H NMR spectrum in $CDCl_3$ for the isolate cyanide **3f** of the photocatalytic oxidative cyanation of amine (**1f,** 20 mM) in the presence of the photocatalyst **[Ru3]Cl$_2$** (1 mol%) in CH_3CN under O_2 and blue LED irradiation (λ_{exc} = 460 nm) at room temperature.

3a: 2-(benzylamino)-2-phenylacetonitrile

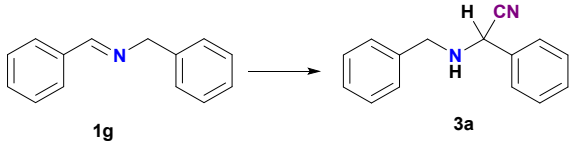

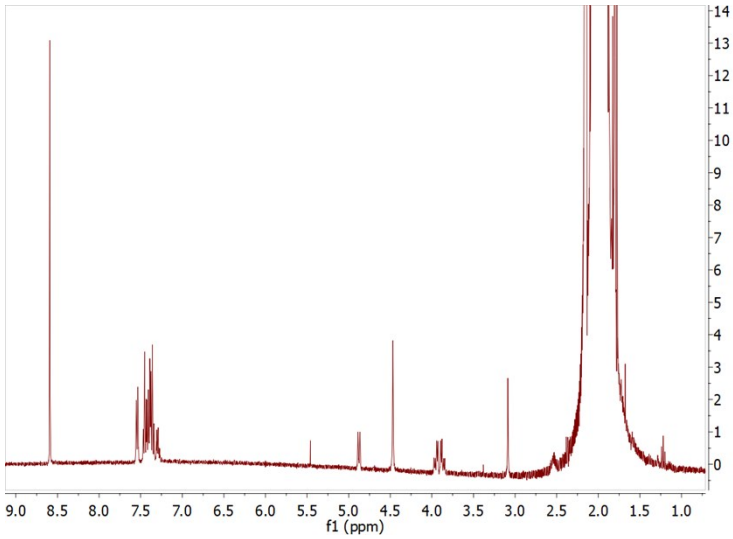

Figure SI26. ^{1}H NMR spectrum in CD_3CN for the crude **3a** of the photocatalytic oxidative cyanation of amine (**1g,** 20 mM) in the presence of the photocatalyst **[Ru3]Cl$_2$** (1 mol%) in CH_3CN under O_2 and blue LED irradiation (λ_{exc} = 460 nm) at room temperature

3h: 2-(hexylamino)heptanenitrile

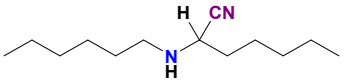

^{1}H NMR (400 MHz, $CDCl_3$, 25 °C) δ 3.50 (t, J = 7.1 Hz, 1H), 2.91 – 2.80 (m, 1H), 2.60 (ddd, J = 11.0, 8.0, 6.2 Hz, 1H), 1.73 (p, J = 7.3, 6.8 Hz, 2H), 1.58 – 1.40 (m, 4H), 1.40 – 1.20 (m, 10H), 1.07 (s, 1H), 0.95 – 0.80 (m, 6H) ppm. **HR ESI+ MS (CH_2Cl_2 4:1):** [M+H$^+$] calcd. for $[C_{13}H_{27}N_2]^+$ 211.2174, found 211.2173.

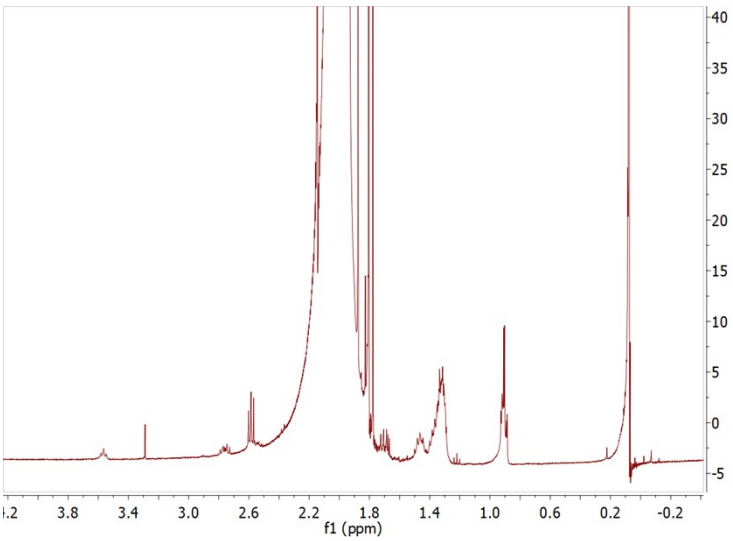

Figure SI27. ^{1}H NMR spectrum in CD_3CN for the crude **3h** of the photocatalytic oxidative cyanation of amine (**1h,** 20 mM) in the presence of the photocatalyst **[Ru3]Cl_2** (1 mol%) in CH_3CN under O_2 and blue LED irradiation (λ_{exc} = 460 nm) at room temperature.

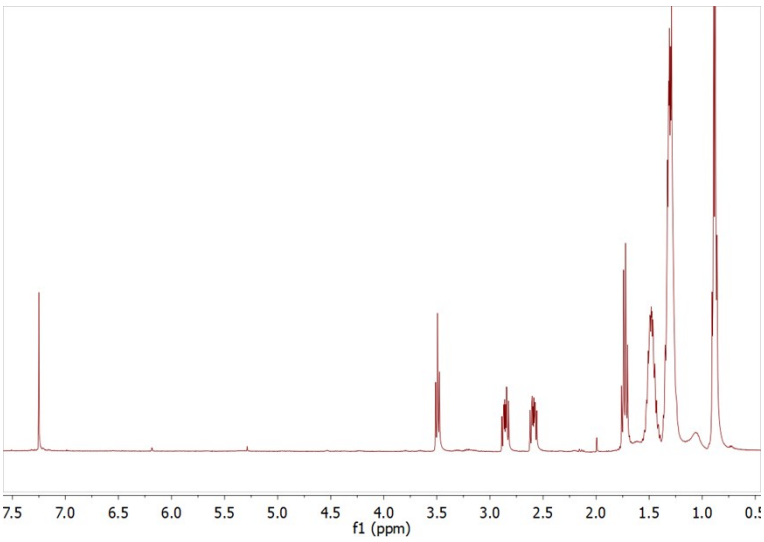

Figure SI28. ^{1}H NMR spectrum in $CDCl_3$ for the isolate cyanide **3h** of the photocatalytic oxidative cyanation of amine (**1h,** 20 mM) in the presence of the photocatalyst **[Ru3]Cl_2** (1 mol%) in CH_3CN under O_2 and blue LED irradiation (λ_{exc} = 460 nm) at room temperature.

3i: 1,2,3,4-tetrahydroisoquinoline-1-carbonitrile

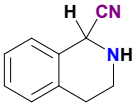

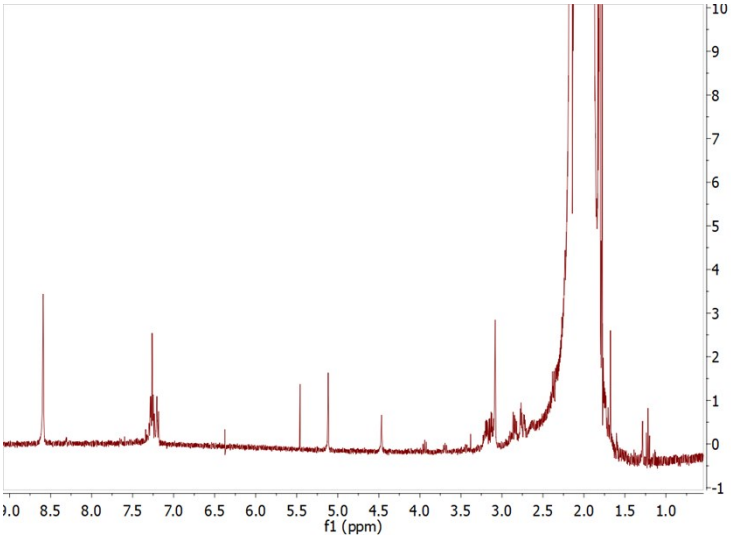

Figure SI29. ^{1}H NMR spectrum in CD_3CN for the crude **3i** of the photocatalytic oxidative cyanation of amine (**1i,** 20 mM) in the presence of the photocatalyst **[Ru3]Cl$_2$** (1 mol%) in CH_3CN under O_2 and blue LED irradiation (λ_{exc} = 460 nm) at room temperature

3j: 2-(thiophen-2-yl)-2-((thiophen-2-ylmethyl)amino)acetonitrile

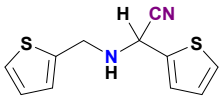

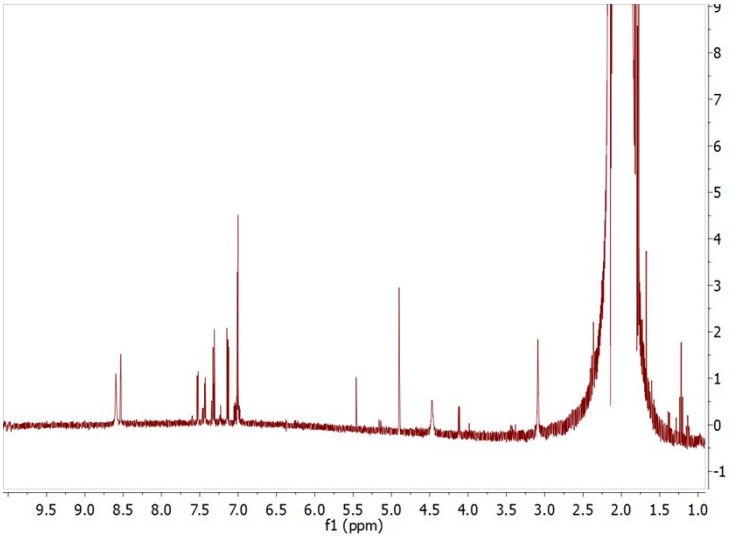

Figure SI30. ^{1}H NMR spectrum in CD_3CN for the crude **3j** of the photocatalytic oxidative cyanation of amine (**1j**, 10 mM) in the presence of the photocatalyst **[Ru3]Cl$_2$** (1 mol%) in CH_3CN under O_2 and blue LED irradiation (λ_{exc} = 460 nm) at room temperature.

3k: 2-((2-methylbenzyl)amino)-2-(o-tolyl)acetonitrile

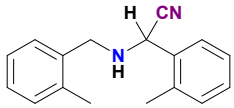

^{1}H NMR (400 MHz, $CDCl_3$, 25 °C) δ 7.63 – 7.55 (m, 1H), 7.33 (d, J = 7.1 Hz, 1H), 7.30 – 7.22 (m, 2H), 7.22 – 7.14 (m, 4H), 4.83 (d, J = 8.9 Hz, 1H), 4.08 (d, J= 13.6 Hz, 1H, CH_2), 3.94 (d, J= 13.6 Hz, 1H, CH_2), 2.38 (s, 3H), 2.29 (s, 3H) ppm.

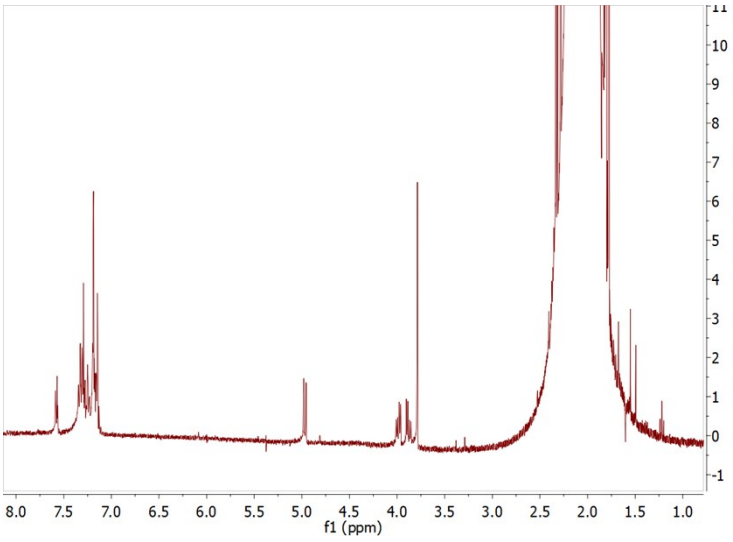

Figure SI31. ^{1}H NMR spectrum in CD_3CN for the crude **3k** of the photocatalytic oxidative cyanation of amine (**1k**, 20 mM) in the presence of the photocatalyst **[Ru3]Cl$_2$** (1 mol%) in CH_3CN under O_2 and blue LED irradiation (λ_{exc} = 460 nm) at room temperature

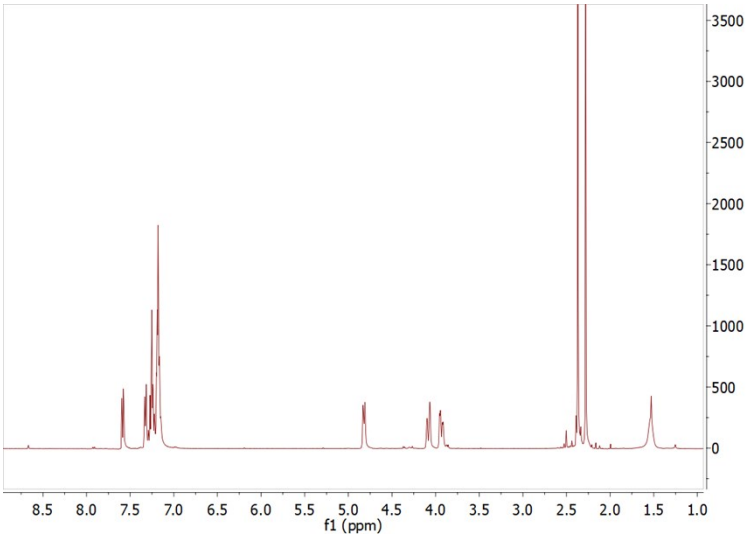

Figure SI32. ^{1}H NMR spectrum in $CDCl_3$ for the isolate cyanide **3k** of the photocatalytic oxidative cyanation of amine (**1k,** 20 mM) in the presence of the photocatalyst **[Ru3]Cl$_2$** (1 mol%) in CH_3CN under O_2 and blue LED irradiation (λ_{exc} = 460 nm) at room temperature.

12.- Detection of by-products in photocatalytic experiments

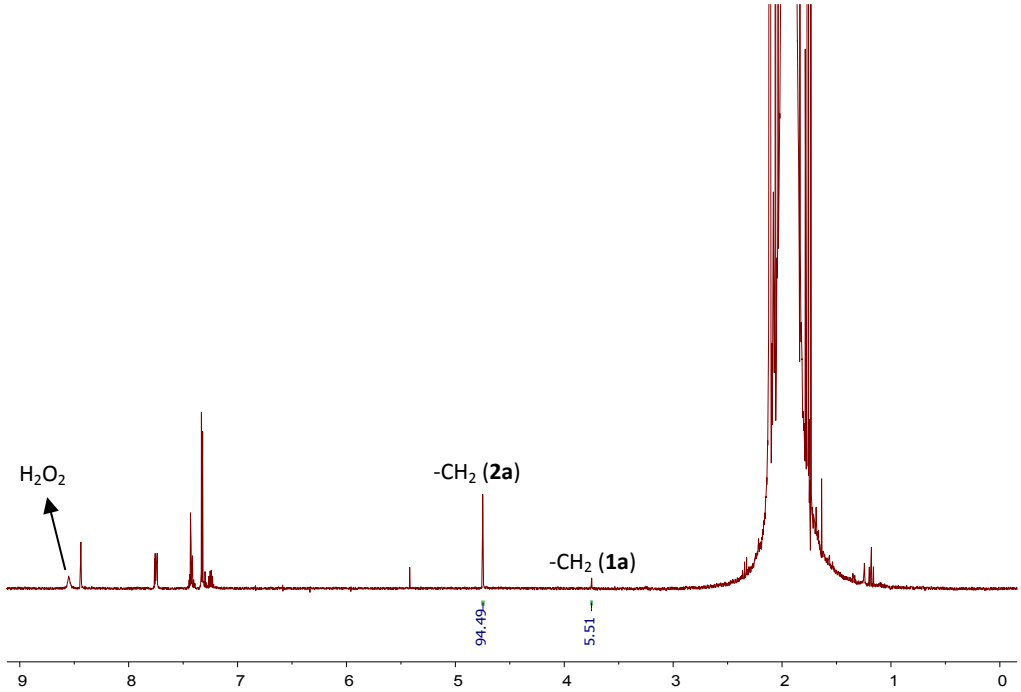

Figure SI33. ^{1}H NMR spectra in CD_3CN at 25 °C of the crude mixture obtained for the photocatalytic oxidative coupling of **1a** to produce **2a**, in the presence of **[Ru3]Cl$_2$** (1 mol %), showing a broad singlet for H_2O_2.

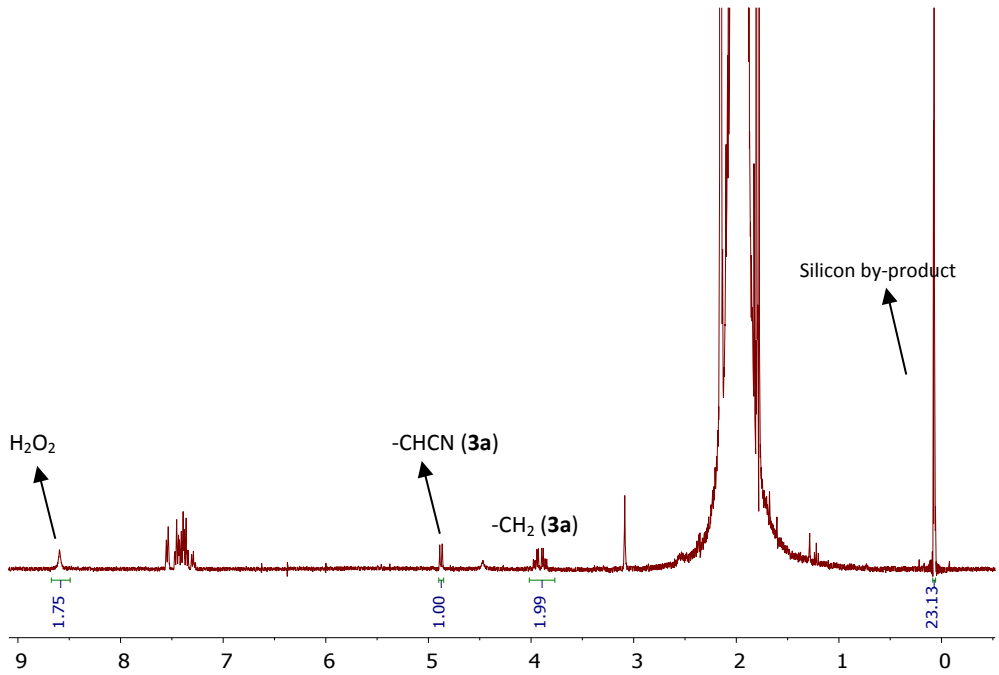

Figure SI34. ^{1}H NMR spectrum in CD_3CN at 25 °C of the crude mixture obtained for the photocatalytic oxidative cyanation of **1a** to give **3a**, , in the presence of **[Ru3]Cl$_2$** (1 mol %), showing signals attributed to H_2O_2 and likely to Me_3SiOH.

Figure SI35. a) Detection of H_2O_2 using Quantofix® peroxide sticks (range 0-25 mg/L H_2O_2, Sigma-Aldrich) for semiquantitative determination of peroxide. The stick was introduced in the crude mixture of a photocatalytic experiment (photooxidation of benzylamine, **1a**, in the presence of **[Ru3]Cl$_2$** (1 mol %)) after 30 min of reaction and turned blue as a symptom of H_2O_2 presence, b) Control experiment, c) Non used stick.

13. 10-fold scale-up

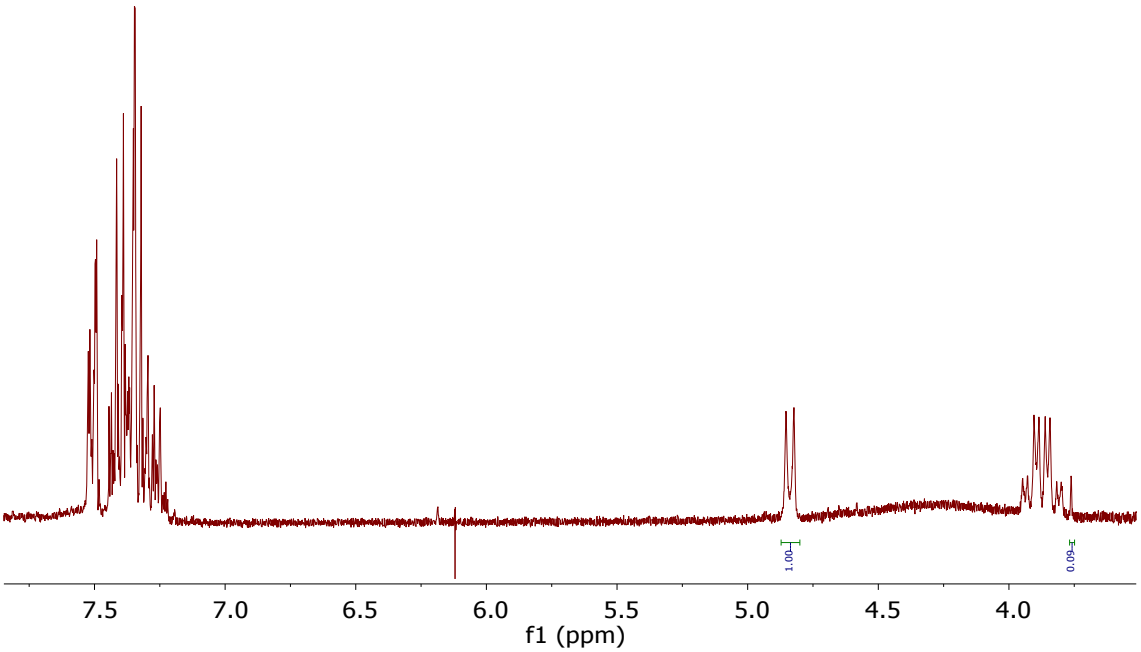

Figure SI36. ^{1}H NMR spectrum in CD_3CN at 25 °C of the crude mixture obtained for the photocatalytic oxidative cyanation of **1a** (200 mg, 1.87 mmol) with TMSCN (2 equiv) in CH_3CN (25 mL) to give **3a** (96 % yield), in the presence of **[Ru3]Cl$_2$** (1 mol %), under O_2 (1 atm) after 6 h of irradiation with stirring at room temperature. The singlet observed at 3.75 is attributed to the benzylamine **1a** (4 %).

14. Photooxidative coupling of 1a to produce 2a using [Ru3]Cl_2 (0.1 mol %)

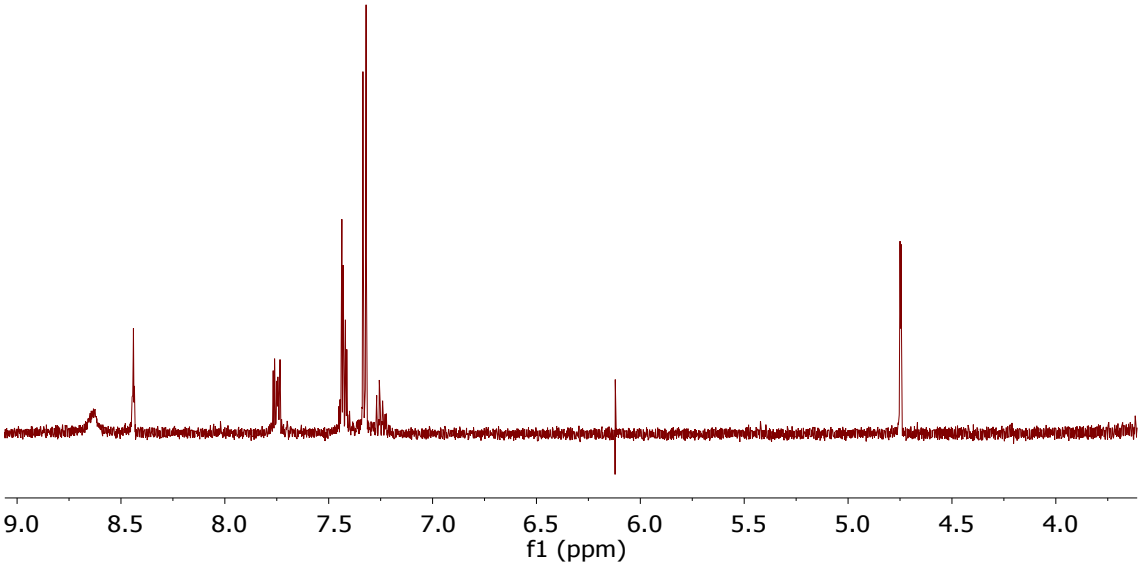

Figure SI37. ^{1}H NMR spectra in CD_3CN at 25 °C of the crude mixture obtained for the photocatalytic oxidative coupling of **1a** to produce **2a**, in the presence of **[Ru3]Cl_2** (0.1 mol %) under 2 h of irradiation with blue light (LED, 460 nm, 24 W).